

# **In vitro and in vivo osteogenic potential of niobium-doped 45S5 bioactive glass: A comparative study**

*‡João H. Lopes\*, ‡Lucas P. Souza\*, Juliana A. Domingues, Filipe V. Ferreira, Moema de Alencar Hausen, José A. Camilli, Richard A. Martin, Eliana Aparecida de Rezende Duek, Italo O. Mazali, Celso A. Bertran.*

## **AUTHOR INFORMATION**

### **J. H. Lopes**

Department of Chemistry, Division of Fundamental Sciences (IEF), Aeronautics Institute of Technology (ITA), 12228-900, Sao Jose dos Campos-SP – Brazil.

E-mail: ([lopes@ita.br](mailto:lopes@ita.br))

### **L. P. Souza (corresponding author)**

Department of Structural and Functional Biology, Institute of Biology, University of Campinas – UNICAMP, 13083-862, Campinas, SP, Brazil.

E-mail: ([lpls2002@hotmail.com](mailto:lpls2002@hotmail.com))

### **J. A. Domingues**

Department of Structural and Functional Biology, Institute of Biology, University of Campinas – UNICAMP, 13083-862, Campinas, SP, Brazil.

E-mail: ([almeidajad\\_bio@hotmail.com](mailto:almeidajad_bio@hotmail.com))

### **F. V. Ferreira**

School of Chemical Engineering, University of Campinas - UNICAMP, 13083-970, Campinas, SP, Brazil.

E-mail: ([filipevargasf@gmail.com](mailto:filipevargasf@gmail.com))

### **M. A. Hausen**

Department of Physiological Sciences, Biomaterials Laboratory, Pontifical Catholic University of São Paulo - PUC- SP, 18030-070, Sorocaba, SP, Brazil

E-mail: ([mahausen@pucsp.br](mailto:mahausen@pucsp.br))

### **J. A. Camilli**

Department of Structural and Functional Biology, Institute of Biology, University of Campinas – UNICAMP, 13083-862, Campinas, SP, Brazil.

E-mail: ([jcamilli@unicamp.br](mailto:jcamilli@unicamp.br))

### **R. A. Martin**

School of Engineering & Aston Research Centre for Healthy Ageing, Aston University, B47ET Birmingham, United Kingdom.

E-mail: ([r.a.martin@aston.ac.uk](mailto:r.a.martin@aston.ac.uk))

### **E. A. R. Duek**

Department of Physiological Sciences, Biomaterials Laboratory, Pontifical Catholic University of São Paulo - PUC- SP, 18030-070, Sorocaba, SP, Brazil

E-mail: ([eliduek@pucsp.br](mailto:eliduek@pucsp.br))

### **I. O. Mazali**

Department of Inorganic Chemistry, Institute of Chemistry, University of Campinas – UNICAMP,  
P.O. Box 6154, 13083-970, Campinas, SP, Brazil.

E-mail: ([mazali@iqm.unicamp.br](mailto:mazali@iqm.unicamp.br))

**C. A. Bertran**

Department of Physical Chemistry, Institute of Chemistry, University of Campinas – UNICAMP, P.O.  
Box 6154, 13083-970, Campinas, SP, Brazil.

E-mail: ([bertran@iqm.unicamp.br](mailto:bertran@iqm.unicamp.br))

<sup>‡</sup> *These authors contributed equally.*

## Abstract

In vitro and in vivo experiments were undertaken to evaluate the solubility, apatite-forming ability, cytocompatibility, osteostimulation, and osteoinduction for a series of Nb-containing bioactive glass (BGNb) derived from composition of 45S5 Bioglass<sup>®</sup>. Inductively coupled plasma optical emission spectrometry (ICP-OES) revealed that the rate at which Na, Ca, Si, P and Nb species are leached from the glass decrease with the increasing concentration of the niobium oxide. The formation of apatite as a function of time in simulated body fluid was monitored by <sup>31</sup>P MAS NMR spectroscopy. Results showed that the bioactive glasses: Bioglass 45S5 (BG45S5) and 1 mol%- Nb- containing-bioactive glass (BGSN1) were able to grow apatite layer on their surfaces within 3 hours, whilst glasses with higher concentrations of Nb<sub>2</sub>O<sub>5</sub> (2.5 and 5 mol%) took at least 12 hours. Nb-substituted glasses were shown to be compatible with bone marrow-derived mesenchymal stem cells (BMMSCs). Moreover, the bioactive glass with 1 mol% Nb<sub>2</sub>O<sub>5</sub> significantly enhanced cell proliferation after four days of treatment. Concentrations of 1 and 2.5 mol% Nb<sub>2</sub>O<sub>5</sub> stimulated osteogenic differentiation of BM-derived MSCs after 21 days of treatment. For the in vivo experiments, trial glass rods were implanted into circular defects in rat tibia in order to evaluate their osteoconductivity and osteostimulation. Two morphometric parameters were analyzed: (i) thickness of new-formed bone layer and (ii) area of new-formed subperiosteal bone. Results showed that BGNb bioactive glass is osteoconductive and osteostimulative. Therefore, these results indicate that Nb-substituted glass is suitable for biomedical applications.

**Keywords:** Bioactive glass, niobium, osteostimulation, osteoinduction, bone regeneration

## Introduction

Musculoskeletal disorders are the most widespread human health issue with bone fractures one of the most debilitating.<sup>[1]</sup> Recent investigations showed that men and women aged 50-64 account for nearly 30% of most types of fractures. Furthermore, most tibia fractures occur in working-age individuals. Therefore, fractures not only compromise the quality of life of people but also represent an economic burden due to the medical costs associated with fracture repair, the related lost work productivity and disability to the working age population.<sup>[1,2]</sup>

The progressive increase in the number of fractures has prompted the development of synthetic materials for bone replacement.<sup>[3,4]</sup> Currently, the most widespread treatments for bone replacement include autologous bone, allografts, xenografts, and various types of biomaterials.<sup>[3]</sup> Autologous bone is considered a gold standard for the treatment of large fractures but presents some drawbacks, such as donor site morbidity, limited availability, and some degree of resorption. Both allografts and xenografts possess potential risk of disease transmission, unpredictable resorption rate, and graft rejection. To overcome these challenges, synthetic materials have been developed, and bioactive glass-ceramics are therefore of great importance.<sup>[3,5-8]</sup>

The second generation of biomaterials was defined by their ability to interact with biological environment to enhance tissue bonding as well as progressively degrade while the new tissue regenerates and heals (e.g. hydroxyapatite).<sup>[9]</sup> Today, we are in the era of third generation of biomaterials, which have the additional ability to stimulate specific cellular responses at the molecular level (e.g. Bioglass<sup>®</sup> 45S5).<sup>[9-11]</sup>

The first biomaterial of the third generation was the Bioglass<sup>®</sup> 45S5.<sup>[12,13]</sup> This biomaterial is a glass that is biocompatible and also forms bonds with hard and soft tissues, which ultimately optimizes the stability and lifespan of implants. Many investigations describe several biological properties of Bioglass<sup>®</sup> 45S5, such as angiogenesis, osteostimulation, osteoconduction, and osteoinduction, which are essential for a biomaterial for bone replacement.<sup>[9]</sup> These effects on living

tissues are determined by the chemical composition of the glass. Hence, several researchers have been designing variations of the original Bioglass<sup>®</sup> 45S5 in order to improve its mechanical and biological performance.<sup>[5, 7, 9, 10, 14-18]</sup>

Recent investigations reported the ability of niobium to optimize mechanical and biological performance of synthetic implants.<sup>[1, 3, 10, 14-16, 19]</sup> Niobium first appeared in biomaterials as a component of metallic alloys.<sup>[20]</sup> The introduction of Nb in alloys substituting vanadium, for instance, was shown to enhance biocompatibility.<sup>[21]</sup> In one study Nb-2Zr was reported to exhibit excellent corrosion resistance, fatigue strength, and crack propagation in simulated body fluids.<sup>[21, 22]</sup> It is noteworthy that Nb<sub>2</sub>O<sub>5</sub> is an effective nucleating agent and generally leads to the development of glass-ceramic in silica-poor compositions, such as Bioglass<sup>®</sup> 45S5.<sup>[12]</sup>

In one of our previous studies, we studied two series of bioactive glasses derived from 45S5 Bioglass<sup>®</sup> composition (SiO<sub>2</sub>-Na<sub>2</sub>O-CaO-P<sub>2</sub>O<sub>5</sub>-Nb<sub>2</sub>O<sub>5</sub> system) by multinuclear solid-state NMR under MAS conditions and Raman spectroscopy, which provided a direct experimental insight into the glass structure. We concluded that Nb<sub>2</sub>O<sub>5</sub> (NbO<sub>6</sub> octahedra) predominantly participates in the silicate network by breaking the Si-O-Si bonds to form structures, such as -Si-O-Nb-O-Si- chains, whereas the Nb-O-P bonds would occur in the terminal sites.<sup>[16, 23, 24]</sup> These alterations modified the glass dissolution rate and magnitude, which is believe increases the lixiviation of species with biological importance such as Si, Ca, Na, and Nb.<sup>[24, 25]</sup> Some recent investigations incorporated niobium into the structure of fluorapatites and phosphate-inverted glass and tested their cytocompatibility, osteostimulation and osteoinduction.<sup>[14, 15]</sup> They observed that the presence of niobium resulted in greater biocompatibility and enhanced bioactive properties.<sup>[3, 14, 15]</sup> Furthermore, osteogenic differentiation of human Mesenchymal Stem Cells (hMSCs) was achieved after 21 days of culture on Nb-doped fluorapatite glass-ceramics.<sup>[3]</sup> Even though Nb-substituted silicate glass appears to possess interesting bioactive properties, its effect over pluripotent cells and bone regeneration has not been investigated so far.

Previous studies have investigated the biological effect of substituting niobium pentoxide for phosphorous pentoxide within the glassy matrix.<sup>[26]</sup> The present study is the first investigation to evaluate the properties of the bioactive glass whereby niobium pentoxide is partially substituted for silicon dioxide. *In vitro* and *in vivo* experiments were carried out to assess the bioactivity of the niobium doped bioactive glass with 45S5 as the control glass. For the *in vivo* assay glass rods with and without niobium pentoxide were implanted into circular defects in rat tibia and bone formation was quantified. The *in vitro* experiments consisted of treating bone-marrow-derived mesenchymal stem cells (BMMSCs) isolated from rats with the dissolution products from the glass and verifying their viability and osteogenic differentiation. It also investigated the leaching profile of Si, Ca, Na, P, and Nb species from the bioactive glass using inductively coupled plasma optical emission spectrometry (ICP-OES) as well as the kinetics of apatite formation using high resolution magic angle spinning and solid-state NMR spectroscopy method to explore the <sup>31</sup>P chemical environments.

## **Experimental**

### ***Preparation of niobium doped bioactive glass samples***

The glass compositions were prepared using a traditional melt-quenching technique since it is the most widespread method used to produce the currently commercialized bioactive glasses.<sup>[12, 27, 28]</sup> The detailed process of preparation of bioactive glass samples is described in our previous publication.<sup>[16, 26]</sup> In brief, high purity SiO<sub>2</sub>, Na<sub>2</sub>CO<sub>3</sub>, CaCO<sub>3</sub>, P<sub>2</sub>O<sub>5</sub> powders (>99.9%) were purchased from Sigma-Aldrich (St. Louis, MO, USA) except for the niobium oxide (Nb<sub>2</sub>O<sub>5</sub>) that was donated by the CBMM (*Companhia Brasileira de Metalurgia e Mineração, Araxá, Minas Gerais, Brazil*). The precursors were mixed and ground in a high-energy mill to homogenize, before transferring into a platinum crucible and heating to 950°C for 3 h with a heating rate of 5 °C.min<sup>-1</sup> to decompose the carbonates and form oxides. P<sub>2</sub>O<sub>5</sub> was added just before the melting process begins. Thirty-gram batches were melted in a platinum crucible at 1400°C in air for 3 h with a heating rate of 10 °C.min<sup>-1</sup> using a Lindberg/Blue M 1700°C furnace (model BF51524C). The melt was poured onto a cylindrical

graphite mold. The prepared glasses were immediately transferred to another furnace maintained at 500°C for annealing and relieving the thermal stresses for 12 h in air before being slowly cooled to room temperature ( $1^{\circ}\text{C}\cdot\text{min}^{-1}$ ) to obtain the glass compositions depicted in **Table 1**.

---

INSERT TABLE 1

---

The niobium oxide was donated by the CBMM (*Companhia Brasileira de Metalurgia e Mineração, Araxá, Minas Gerais, Brazil*). The glasses were ground and sieved to isolate the desired particle size (between 38 $\mu\text{m}$  and 53 $\mu\text{m}$ ). For the *in vivo* studies cylindrical rods with 4 mm length x 2 mm diameter were prepared by casting method using appropriate graphite molds (see the **Topic SM1**).

***Ionic leaching patterns of bioactive glass by ICP-OES***

Inductively coupled plasma optical emission spectrometry (ICP-OES) was used to verify the ionic leaching patterns of bioactive glass particles. In brief: 300 mg of bioactive glass particles were dispersed in a beaker with 200 mL of buffer solution and maintained under continuous stirring (stirring rate of 75 rpm), at room temperature. Using a 50.69 mM HEPES (2-(4-(2-hydroxyethyl)piperazin-1-yl)ethanesulfonic acid) (Sigma-Aldrich, St. Louis, MO, USA) and 1 mM NaOH (Sigma-Aldrich, St. Louis, MO, USA) the solution pH was adjusted to 7.40. The solution was filtered using a 0.22  $\mu\text{m}$  pore filter (Millipore<sup>®</sup>) in order to remove contaminants and aggregates. The glass was then added to the solution and allowed to mix for 3, 6, 12, 24 and 48 hours. At each time point 10 mL of solution was collected with a syringe and passed through a 0.22  $\mu\text{m}$  pore filter (Millipore<sup>®</sup>) and analyzed with an ICP-OES spectrometer (Optima 8300 ICP-OES, PerkinElmer, Inc., Shelton, CT, USA). Three replicates were measured for each element.

***Analysis of the calcium phosphate layer by  $^{31}\text{P}$  MAS NMR spectroscopy***

$^{31}\text{P}$  MAS NMR was performed to analyze the rate of formation of the calcium phosphate layer on the bioactive glass surfaces. Samples of 50 mg of bioactive glass particles were added to 5 mL of simulated body fluid (SBF) (see the **Topic SM2 – Table SM1**) and the mixture was stirred in a thermostatic bath at 37 °C. After 3, 12, 24 and 48 hours the solution was filtered and the remaining

powder was immediately dried between two filter papers. Soon after the drying procedure the material was packaged into a 4-mm cylindrical zirconia rotor and spun at the MAS frequency at the magic angle to remove any anisotropy effect. The samples were spun at 10 kHz. The  $^{31}\text{P}$  MAS spectra were obtained using a high-power decoupling (HPDEC) pulse sequence with 2.50  $\mu\text{s}$  pulses, 82 ms acquisitions, 5s recycle delays, a 100 kHz spectral width, and 1024 scans. The  $^{31}\text{P}$  chemical shifts were referenced to 85%  $\text{H}_3\text{PO}_4$ . The spectra were processed with TopSpin 2.1.6 software using Fourier transforms and an exponential filter of 50 Hz. The phase was manually adjusted, and the baseline was obtained using a five-order polynomial function. This experiment was performed in triplicate.

### ***Culture of BM derived Mesenchymal Stem Cells (MSCs)***

Bone marrow derived Mesenchymal Stem Cells (BMMSCs) were isolated from the tibia and femoral of five adult Wistar rats weighing 250 - 300g. For this, the bone epiphyses were removed and discarded. The bone shafts were centrifuged at 1500 rpm for 15 minutes in order to precipitate their bone marrows. The pellet (composed by the precipitated bone marrow) was re-suspended in Dulbecco's modified Eagle's medium (DMEM) supplemented with 1 % penicillin/streptomycin solution and 10 % fetal bovine serum (FBS) (complete DMEM) in a 37 °C / 5 %  $\text{CO}_2$  incubator. Cells, up to their fourth passage, were maintained in supplemented DMEM. All media were changed every other day.

### ***Cell viability – MTT assay***

Cytotoxicity was analyzed using 3-(4,5-dimethylthiazol-2-yl)-2,5-diphenyltetrazolium bromide (MTT) assay (Sigma-Aldrich, St. Louis, MO, USA). For this, 5000 BMMSCs were cultured in conditioned media containing 10  $\text{mg}\cdot\text{mL}^{-1}$  of each of the glass compositions (BG45S5, BGSN1, BGSN2.5 and BGSN5), for a period of four days. Cells grown in complete DMEM served as a positive control while cells previously incubated in Dimethyl sulfoxide (DMSO) for 30 minutes served as a negative control. The MTT assay was performed following the manufacturer's instructions. In short, 12 mM stock solution of MTT was prepared and diluted 10 x in phenol red free medium before being

added to the cells, which were incubated for 4 h at 37 °C. After the incubation 75 µL of medium was replaced by 50 µL of Dimethyl sulfoxide (DMSO) and left to incubate at 37 °C for 10 min. MTT was reduced to formazan by metabolically active cells and the optical density was measured using a spectrophotometer (at 570 nm). This assay was performed in quintuplicate.

#### ***Cell viability – Live/Dead assay***

10,000 BM- derived MSCs were seeded per well and treated for 72 h with conditioned media containing the dissolution products of 45S5 Bioglass<sup>®</sup>, BGSN1, BGSN2.5 and BGSN5 at a concentration of 10 mg·mL<sup>-1</sup>. Following the incubation period, a negative control of dead cells was established by incubating cells with 70% methanol for 30 min. Cells treated with regular growth media served as a positive control. The polyanionic dye calcein-green is retained within live cells, producing an intense uniform green fluorescence. Ethidium homodimer-1 (EthD-1) enters cells with damaged membranes and undergoes a 40-fold enhancement of fluorescence upon binding to nucleic acids, thereby producing a bright red fluorescence in dead cells. To stain BM- derived MSCs working concentrations of calcein-green at 2 µM and EthD-1 at 4 µM were combined into one solution and used to treat cells. Cells were overlaid with 200 µL of staining solution. For this assay five wells of cells were used per group.

#### ***Staining mineralized nodules with Alizarin Red 1%***

BM-derived MSCs were cultured in complete medium until a monolayer was formed (~10 days). Following the formation of the monolayer cells were treated for three weeks with one of the experimental media: (a) complete DMEM; (b) osteogenic medium, composed of complete DMEM supplemented with 0.1 mM ascorbic acid, 3mM β-Glycerolphosphate and 10<sup>-8</sup> M dexamethasone (Sigma-Aldrich, St. Louis, MO, USA); (c) BGSN1 (complete DMEM + 10mg/mL of BGSN1); (d) BGNS2.5 (complete DMEM + 10mg/mL of BGSN2.5; or (e) BGSN5 (complete DMEM + 10mg/mL BGSN5). After 21 days of incubation the monolayers were stained with Alizarin Red 1% (Sigma-Aldrich, St. Louis, MO, USA) in order to analyze the presence of mineralized nodules, which is a

marker of osteogenic differentiation. In short, cell monolayers were fixed with 70% ethanol for 1 hour at 4 °C and incubated in 1% Alizarin Red for 10 minutes. The plates were then washed five times with distilled water and microphotographs at 100 x magnification were taken from each well. Five wells were used per group.

### ***Immunofluorescence for Osteocalcin***

20,000 BM- derived MSCs were cultured per well. Cells were treated for 21 days with culture media conditioned with the dissolution products of BG45S5 and BGSN1. Cells treated with osteogenic medium (StemPro™ Osteogenesis Differentiation Kit, ThermoFisher) were used as a positive control. After 21 days of treatment cells were fixed with 4% paraformaldehyde for 30 minutes and treated with a 0.25% solution of Triton X-100 for 30 minutes. Cells were then incubated in Osteocalcin primary antibody (Abcam) at 1:100 for 1 hour at room temperature. After washing with saline solution, cells were incubated in the secondary antibody (Alexa-Fluor 647 goat to rat, Abcam) for 1 hour at room temperature. The cellular nucleuses were stained with DAPI. Images were obtained with a Laser Scanning Confocal Microscope (LSCM, Leica TCS SP5) in PMT mode. Reflection images of laser in TRANS mode were obtained in order to identify mineralized matrix. This experiment was performed in triplicate.

### ***Atomic force microscopy (AFM)***

Surface roughness of bioactive glasses before and after immersion in culture medium was measured by atomic force microscopy (AFM) using a NX-10 atomic force microscope (Park System) operating on intermittent contact. The nominal spring constant and resonant frequency of the silicon tip (Nanosensors) were 42 N/m and 320 kHz, respectively. Firstly, the bioactive glass discs were polished in a similar way and immersed in culture medium and maintained at 37 °C for 24 hours. Then, the samples were allowed to completely dry for 48 hours at room temperature. The images were recorded at room temperature and Gwyddion software was used to process the AFM images. The root

mean square (RMS) surface micro-roughness was obtained on 30 x 30  $\mu\text{m}$  scans. This experiment was performed in triplicate.

### ***Scanning electron microscopy (SEM)***

The surface roughness was qualitatively characterized by scanning electron microscopy (SEM) using FEI Inspect F50 available at LNNano, Campinas. The operating voltage and working distance were 20 kV and 10.5 mm, respectively. The samples before and after immersion in culture medium were fixed on a metal stub using carbon tape and coated with gold before observations. This assay was performed in triplicate.

### ***In vivo analysis***

Glass rods were implanted into rat tibia. For this, Brazilian College of Animal Experimentation (BCAE) guidelines were followed, and experiments were approved by Ethics Committee in Animal Use – ECAU/Unicamp (**Protocol n° 2777-1**). Rods composed of BG45S5 or BGNS1 were implanted into a round defect created in the tibia of rats that had been anesthetized with a mixture of ketamine (ANASEDAN<sup>®</sup>) at 80  $\text{mg}\cdot\text{kg}^{-1}$  and xylazine (DOPALEN<sup>®</sup>) at 10 $\text{mg}\cdot\text{kg}^{-1}$ . Five rats were used per group. A round transcortical defect was created using a spherical threfine bur (JET<sup>®</sup>) with a diameter of 2 mm after pulling aside the periosteum. The glass rod (4 mm length x 2 mm diameter) was carefully introduced into the defect until total coupling, then the periosteum and the skin were sutured. After 28 days, the animals were euthanized, and the tibia was obtained from the animals and fixed for 24 h at 4 °C in 10% zinc-buffered formalin (Sigma-Aldrich, St. Louis, MO, USA). After fixation, they were decalcified in 5% EDTA (Synth Labsynth, Diadema, SP, Brazil), the glass rod was then carefully removed and the bones were paraffin-embedded and sectioned.

### ***Morphometry***

All histological slides were stained with hematoxylin and eosin dyes and a light microscope (Nikon 80i model, Nikon Corporation, Tokyo, Japan) with a camera Nikon Model DS-Ri1 and NIS-Elements software: Advanced Research 3.0 were used to quantify: (i) area of new-formed subperiosteal

bone and (ii) thickness of new-formed bone layer. For each quantification five rats per group were used.

### *Statistical Analysis*

A comparison between the mean values of subperiosteal new formed bone and of the thickness of the bone layer formed around the implant were undertaken using an ANOVA one-way test with tukey (homogeneous variances) or Games-Howell (non-homogeneous variances) post-hoc. For all tests  $\alpha = 0.05$  was assumed. All data are described using the mean and standard error.

## **Results and discussion**

### *Dissolution studies*

**Figure 1** illustrates the release of Na, Ca, Si and P from the glass and **Figure 2** shows the concentration of Nb species as determined by inductively coupled plasma optical emission spectrometry (ICP-OES). The release of soluble ions from bioactive glasses is known to be the key first step in the bio-mineralization process as described by Clark and Hench.<sup>[11, 12, 29]</sup>

---

### INSERT FIGURE 1

---

The release of Ca and P creates a supersaturated solution which then precipitates into amorphous calcium phosphate which then crystallizes in apatite.<sup>[30, 31]</sup> Furthermore, the controlled release of Si, Ca, Na, P, and Nb species from the bioactive glass has been associated with the promotion of bioactivity, angiogenesis, osteostimulation, osteoconduction, and other important properties for bone regeneration.<sup>[2, 9-11]</sup> The BG45S5 bioglass composition is also presented for the purpose of comparison. As shown there is a rapid release of ions following immersion in HEPES solution. From the release of Na and Ca ions (**Figure 1 (a-b)**) it appears at first glance as though the BG45S5 bioglass is the most soluble and that the solubility decreases upon increasing concentrations of Nb. However, it is important to note that the molar mass of Nb<sub>2</sub>O<sub>5</sub> is ~ 4.4 times heavier than SiO<sub>2</sub>. Therefore a 300 mg sample of BGSN5 will contain 15% less CaO, Na<sub>2</sub>O and P<sub>2</sub>O<sub>5</sub> compared to BG45S5. Taking this into consideration and given the errors the release of Ca and Na is similar for the glasses with the

exception of the BGSN5 which is clearly much less soluble. The Si concentrations shows a slight increase in solubility for the 1 and 2.5 mol% Nb glasses despite it having a lower SiO<sub>2</sub> concentration.

The increase in Si solubility is attributed to the degree of matrix fragmentation caused by both the reduction of Si and more importantly the additional oxygen atoms provided by Nb<sub>2</sub>O<sub>5</sub> compared to SiO<sub>2</sub>. The higher the niobium content the more non-bridging oxygen atoms and the greater the number of Si-O-Nb bonds.<sup>[16, 23, 24]</sup>

The release profile of phosphorus suggests a maximum concentration (approximately the solubility limit), from which there is a dramatic reduction, presumably associated with the removal of some of the soluble phosphate species to form the calcium phosphate layer on the bioactive glass surface (**Figure 1d**). The results indicate that an amorphous calcium phosphate is rapidly deposited for BG45S5 and BGSN1, with a delay and a reduction observed for BGSN2.5 whilst BGSN5 appears too insoluble to release sufficient P (or Ca) to begin to form ACP. A characteristic common to all leaching curves for sodium, calcium, silicon, and phosphorus species in the earliest dipping times is the mechanism of the species lixiviation. The initial elemental concentrations up to about 120 min for all compositions are a linear function of the square root of time, which indicates a diffusion-controlled process (see the **Topic SM3**).

The profile shape of niobium species at early soaking times are similar to those observed for P, i.e., a sudden increase in the Nb concentration in the medium, reaching a maximum value, followed by a characteristic reduction of concentration value for each glass (**Figure 2**).

---

#### INSERT FIGURE 2

---

This initial increase is related to the leaching of niobium species near surface and/or release of isolated NbO<sub>6</sub> units, which are more labile since their release does not require extra energy to break bonds in comparison with the Nb-O-Nb groups. The rate at which the niobium species are removed from the solution is gradual and can be mostly attributed to polymerization of the niobate species (Nb-O-Nb), which are continuously subtracted from the medium to form the niobium gel layer on the bioactive glass surface.<sup>[24]</sup> The Nb-OH groups are chemically stable (Brønsted and Lewis acid sites),

as well as effective nucleation centers for the removal of the leached niobium species from the glass.<sup>[16]</sup> Consequently, the concentration of free niobium decreases as the niobium gel layer is established on the surface of the bioactive glass, i.e., the limit solubility of niobium is reduced.

#### *Apatite layer formation ability by <sup>31</sup>P MAS NMR spectroscopy*

Amorphous calcium phosphate / apatite formation on the bioactive glass surface in simulated body fluid (SBF) has been verified by <sup>31</sup>P MAS NMR (**Figure 3 (a-d)**).

---

#### INSERT FIGURE 3

---

As shown the local structural arrangement of phosphorus changes rapidly even for early soaking times.<sup>[7, 24]</sup> The <sup>31</sup>P MAS NMR spectra of unreacted BG45S5, BGSN1, BGSN2.5 and BGSN5 exhibit a single broad resonance around 11 ppm with peak maximum at 11.9, 11.8, 11.6 and 8.5 ppm, respectively. The <sup>31</sup>P resonances are attributed to the  $P^{0-}$  isolated orthophosphate units (charge balanced by  $Na^+$  and  $Ca^{2+}$ ).<sup>[24, 32]</sup> In addition, as the niobium content increases there is a tiny shift to lower frequencies followed by a more significant shift for the BGSN5 suggesting that Nb interacts with phosphorus, presumably forming P-O-Nb bonds. The data extracted from the <sup>31</sup>P MAS NMR spectra such as peak positions and full width half maximums (FWHM) for BG45S5 and Nb-substituted glass, unreacted and after 3, 12, and 24 hours of immersion in in simulated body fluid (SBF) are listed **Table 2**.

---

#### INSERT TABLE 2

---

<sup>31</sup>P MAS NMR data show a trend that describes the evolution in the chemical environment of the phosphorus during the chemical transformations at the bioactive glass solution interface as a function of the soaking time in SBF. All <sup>31</sup>P resonances are characterized by notable shift to lower frequencies during the soaking time in SBF, reaching the frequency of approximately 4 ppm, which is similar to the signal observed in the spectrum of hydroxyapatite. Such spectral changes and the decrease in FWHM values describe the partial degradation of glass and precipitation of amorphous calcium phosphate and its progressive crystallization.<sup>[24]</sup> <sup>31</sup>P MAS NMR spectra for BG45S5 (**Figure**

**3a)** and BGSN1 (**Figure 3b**) suggest that 3 hours of incubation in SBF are enough to establish an ACP/ apatite layer. While for BGSN2.5 glass the time required is considerably longer, approximately 12 hours (**Figure 3c**). Although subtle, the changes observed in the BGSN2.5 spectrum in the range of 13-24 hours are related mainly to the gradual increase in the crystallinity of calcium phosphate (increase of long-range order). In contrast, <sup>31</sup>P MAS NMR spectrum for the BGSN5 exhibit a progressive increase in the FWHM values of the resonance peak as a function of the soaking time in SBF (**Figure 3d**). This is a result of some P remaining in the glass network at ~1 ppm whilst some P starts to form an ACP/ apatite precipitated on the glass surface ~4 ppm resulting in a much wider distribution of frequencies. For the BG45S5, BGSN1 and BGSN2.5 samples, almost all of the phosphorus present in the glass network is continuously leached into the solution, where it is precipitated in the form of calcium phosphate in the gel layer (silica- and/or niobosilica-gel) formed on the bioactive glass surface.

In summary, all vitreous compositions have been able to form the phosphate layer, but as the niobium content increases the chemical stability of the bioactive glass increases, and the dependence of an external source of phosphorus for apatite composition increases. In accordance with this assumption, <sup>31</sup>P MAS NMR spectra display resonance peaks with a slight asymmetry on the left-hand side of the peak owing to the residual glass fraction.

### ***Cytocompatibility assessment***

Cytocompatibility is essential for all biomaterials. Any sign of toxicity may represent a risk for the recipient organism and therefore must be avoided. In this work we evaluated the cytocompatibility of the dissolution products of different compositions of BGNb glasses (BGSN1, BGSN2.5 and BGSN5) with BG45S5 as the control with rat bone marrow mesenchymal stem cells (BM-MSCs) by MTT and Live/Dead assay. We treated cells with culture media conditioned with the dissolution products of the different glasses for up to four days. Cells treated with complete DMEM were used as positive controls meanwhile cells killed with dimethyl sulfoxide (DMSO) or 70% methanol served as

negative controls. None of the glass-conditioned media was cytotoxic to this cell type (**Figures 4**). This result demonstrates that the incorporation of niobium oxide into the structure of Bioglass<sup>®</sup> 45S5 does not compromise its cytocompatibility.

---

#### INSERT FIGURE 4

---

As it can be seen on **Figure 4g** the viability of cells treated with medium conditioned with the composition BGSN1 were considerably higher than the Bioglass<sup>®</sup> 45S5 glass and the positive control group (complete DMEM) which indicates that this glass enhances cell proliferation. Several other studies have also shown that the addition of niobium into biomaterials do not result in cytotoxicity. These investigations include tests with different materials such as fluorapatite glass-ceramics,<sup>[3]</sup> phosphate glasses,<sup>[33]</sup> bioactive glass-niobium granules,<sup>[19]</sup> hydroxyapatite bioceramics,<sup>[34]</sup> and calcium silicate cements with different cell lines.<sup>[35]</sup> In one of these assays human osteogenic cells (SAOS) were incubated with Nb-doped hydroxyapatite for 72 hours and cell viability was tested by means of a MTT assay. They observed no difference or even a statistically significant increase in cell proliferation when compared to the control group (reference material) which allowed them to conclude that Nb-doped hydroxyapatite has the ability to support cell proliferation.<sup>[34]</sup> Furthermore, a very recent investigation evaluated the cytocompatibility of calcium silicate-based cements combined with niobium oxide (Nb<sub>2</sub>O<sub>5</sub>) micro and nanoparticles, comparing the response in four different cell lines: (a) human dental pulp cells - hDPCs; (b) human dental follicle cells - hDFCs; (c) human osteoblast-like cells (SAOS-2); and (d) mouse periodontal ligament cells - mPDL. After 24 hours of incubation within media conditioned with the materials they measured cellular viability by means of MTT assay. The authors concluded that calcium silicate cements combined with Nb<sub>2</sub>O<sub>5</sub> micro and nanoparticles presented cytocompatibility and can be used as an alternative radiopacifier agent for calcium silicate cements. Therefore, our results complement the existing literature demonstrating that Nb-substituted bioactive glass is cytocompatible and also constitutes a safe biomaterial for biomedical applications.

#### *Osteoinductive potential of Nb-containing glass*

Over the past few years the role of engineered scaffolds complexed with mesenchymal stem cells (MSCs) for bone regeneration has been a main research topic in regenerative medicine.<sup>[36-38]</sup> The bone marrow derived mesenchymal stem cells (BM-MSCs) are multipotent cells that are able to self-renewal and to differentiate into several cell types depending on which chemical or mechanical stimulus they are subjected.<sup>[39]</sup> The bone formation that is required for integration of biomaterials relies on the presence of multipotent cells that are capable of differentiating into osteoblasts.<sup>[39]</sup> As BM-MSCs constitute one of the most abundant multipotent cell types present at the fracture site they play major roles in supporting faster bone formation along implants.

Previous MSCs were complexed with different types of biomaterials such as calcium phosphate<sup>[33, 37]</sup> and biodegradable poly(lactide) (PLA) scaffolds.<sup>[36]</sup> The incorporation of human BM-MSCs in macroporous calcium phosphate cement (CPC) promoted great cell attachment, osteogenic differentiation and mineralization. When these BM-MSCs - containing scaffolds were used to treat cranial defects in rats new bone and blood vessels were generated between 4 and 24 postoperative weeks. In summary, the authors concluded that seeding stem cells with CPC increased new bone and new blood vessel density, compared to CPC without cells, suggesting this material can be used for craniofacial and orthopedic applications.<sup>[37]</sup> In other very recent investigation<sup>[36]</sup> human gingival mesenchymal stem cells (hGMSCs) were cultured with three-dimensional printed PLA scaffolds pre-treated with hGMSCs derived extra cellular vesicles (EVs) in order to test the *in vitro* osteogenic performance of this material by means of alizarin red staining, gene expression of RUNX2 and BMP-2 (RT-PCR), and the concentration of the proteins RUNX2, BMP-2, and  $\beta$ -Actin (Western Blot). The combination of hGMSCs + 3D-PLA + EVs promoted excellent osteogenic differentiation indicating that the combination of pluripotent cells and inorganic scaffolds enhances bone regeneration of cranial defects.<sup>[36]</sup>

The formation of bone requires not only the recruitment and/or migration of potentially osteogenic cells but also their differentiation towards the osteoblastic lineage.<sup>[40]</sup> Scaffolds composed

of BGNb glass may favor MSCs to differentiate into osteoblasts because some investigations have reported that the incorporation of niobium into other types of biomaterials such as fluorapatites and phosphate-inverted glass has incited osteogenic differentiation of hMSCs<sup>[2]</sup> and maturation of mouse osteoblast-like cells (MC3T3-E1 cell).<sup>[14]</sup> The study of Obata and his collaborators<sup>[14]</sup> is of particular importance for the scope of the present work because they tested the osteostimulative capacity of niobium ions over MC3T3-E1 cells. They reported that both ALP activity and calcium deposition of MC3T3-E1 cells was significantly higher in the medium containing niobium at a concentration of  $10^{-7}$  M when compared with control or other Nb-containing media, even though none of the tested media contained osteogenic supplements. The authors proposed that this may indicate that the niobium ions not only enhance but also induce osteogenic differentiation.<sup>[14]</sup>

The osteoinduction capacity of Nb-substituted bioactive glass may result in a higher number of osteoblasts within the implant and consequently at the fracture site. In order to test the capacity of different compositions of BGNb bioactive glass to stimulate the osteogenic differentiation of BM-MSCs we stained mineralized nodules at the extracellular matrix with Alizarin Red after 21 days of treatment with culture media conditioned with the dissolution products of different Nb-containing glasses. We also marked matrix-mineralization-related protein osteocalcin with fluorescent antibody and obtained micrographs using a Laser Scanning Confocal Microscope to demonstrate the presence of this protein which is also a marker of osteogenic differentiation.

The formation of mineralized nodules marks the final step of the process of osteogenic differentiation. In short, this process follows the subsequent stages: (i) proliferation of multipotent cells (as differentiation only progresses after this step we chose to wait for the BM-MSCs to form a monolayer before starting to treat them with the different cell media); (ii) formation of non-mineralized matrix mostly composed of type I collagen; and (iii) mineralization of the matrix forming calcium-rich nodules. Our results showed that the compositions BGSN1 and BGSN2.5 stimulated the formation of nodules comparable to the positive control group (MSCs treated with an osteogenic culture medium)

(**Figure 5, six upper squares**) which is an ultimate sign of osteogenic differentiation. In addition, osteocalcin was present in the bone matrix corroborating previous results (**Figure 5, four lower squares**).

---

INSERT FIGURE 5

---

These results support the claim that Nb-doped bioactive glass may be used to produce highly bioactive scaffolds for bone tissue engineering because they support migration of BM-MSCs and also stimulates osteogenic differentiation of these cells, increasing the population of mature secretory osteoblasts in the fracture site which may hasten bone regeneration.

***Bone formation stimulated by Nb-containing bioactive glasses***

*In vivo* experiments were performed in order to analyze the properties of osteoconductivity and osteostimulation of Nb-containing glass. Osteoconductivity is often referred in the biomaterial literature as the capacity of a material to allow bone to grow onto its surface.<sup>[41]</sup> Despite this definition correctly describing the event it does not explain exactly how it happens. In fact, what makes a new bone form onto a material's surface in a particular direction is the migration of multipotent cells coming from the bone-marrow (bone marrow-derived MSCs), blood (blood-derived MSCs) or, to a lesser extent, from surrounding tissues (e.g. myocytes from the muscles and pericytes from the blood vessels). Just the migratory activity of these cells over the surface responds for the expansion of a bone spicule.<sup>[42]</sup> As soon as a material is placed into a surgically made defect (as in our experiment) it rapidly undertakes a series of ion exchange with the body fluid that culminates with a drastic increase in the surface's roughness (**Figure 6**).

---

INSERT FIGURE 6

---

Rough surfaces are more easily coated with many proteins, lipids, ions, and sugars which will dictate which cell types will subsequently attach.<sup>[42]</sup> It is known that some characteristics of the material's surface, such as its topography, chemical composition, charge, and energy, directly influence protein adsorption and consequently cell adhesion and migration.<sup>[42]</sup> Hence, biomaterials designed for bone replacement must provide a suitable surface for the adhesion and migration of

osteogenic cells that will populate the surface, differentiate into osteoblasts and produce a mineralized matrix.

As the composition BGSN1 showed better performance in the *in vitro* experiments and a significant increase in topographical complexity of its surface it was chosen for the *in vivo* investigation. We implanted glass rods made of BGSN1 into the tibia of rats and examined the formation of a bone layer around the implant. The composition BG45S5 was used as a control. We observed the presence of a bone layer around both glass compositions and calculated their thickness in order to compare the groups (**Figure 7** and **Figure 8**).

---

#### INSERT FIGURE 7

---

In the present work we demonstrate *in vivo* osteoconductivity of Nb-containing bioactive glass. Nevertheless, the ability of other type of niobium-containing materials to support bone growth onto their surfaces was demonstrated *in vivo* by Matsuno and his collaborators.<sup>[43]</sup> They introduced a wire of 99.9% niobium, 1.0 Ø x 7.0mm in size in rat femur bone marrow and evaluated bone formation around the implant after 14 and 28 days. They observed new bone formation onto niobium implant's surface after 28 days, confirming its osteoconductivity.<sup>[43]</sup> In another investigation a cylindrical implant made of Ti-Nb alloy was implanted into medial tibia of beagles for 2, 4 and 12 weeks.<sup>[44]</sup> New bone formation was observed to grow in contact with the material's surface after 4 weeks. In the same study the authors reported that the incorporation of Nb to the metallic alloy increased its surface roughness (Ti-Nb:  $1.79 \pm 0.23 \mu\text{m}$  compared to pure Ti:  $1.63 \pm 0.17 \mu\text{m}$ ) and reduced its contact angle (Ti-Nb:  $81.75 \pm 2.94^\circ$  compared to pure Ti:  $96.46 \pm 3.56^\circ$ ) (more hydrophilic). It is generally accepted that osteogenic cells respond to microroughness ( $<25\mu\text{m}$ ) and tend to adhere to more hydrophilic surfaces.<sup>[45]</sup>

As a matter of fact the surface characteristics determine which types of proteins will adsorb and as a consequence which cell types will be attracted to it.<sup>[42]</sup> Thus, it is believed that the incorporation of Nb into these materials might have provided them with a more suitable surface for

adhesion and maturation of osteogenic cells. A similar mechanism may have been involved in the formation of the bone layer onto BG45S5 and BGNS1.

---

INSERT FIGURE 8

---

We suggest that osteogenic cells coming from the bone marrow and the periosteum contributed to the observed bone formation. As the surface of the material was in direct contact with the periosteum at the outer surface of tibia cortical osteogenic cells could migrate from the periosteum onto material's surface by haptotaxic migratory movement. This pattern of migration is described as a directional motility of cells towards cellular adhesion sites or surface-bound chemoattractants.<sup>[46]</sup> In addition, bone marrow derived MSCs also may have substantially contributed to bone formation attaching to the material's surface probably attracted by its favorable physical, chemical, and/or biological characteristics. The bone formation on the surface reveals that it presented ideal features that favored protein adsorption and consequently cell migration and adhesion followed by subsequent osteogenic differentiation. To confirm this scenario and fully understand the mechanisms underlying the formation of the observed bone layer more comprehensive studies should focus on the characteristics of Nb-containing bioactive glass such as surface topography and hydrophobicity.

It is worth mentioning that direct contact is not the only way by which materials can influence living cells. In fact, inorganic ions were shown to influence formation, regulation and maintenance of bone.<sup>[47]</sup> In our dissolution studies we showed that BGSN1 presents a pattern of ion release very similar to BG45S5 except for the Nb, obviously only found in the Nb-containing glass. The biological roles of BG45S5-derived ions are well described in the literature,<sup>[47, 48]</sup> whereas the role of Nb soluble species over osteogenic cells started to be investigated only recently.<sup>[14]</sup> Ca ions were shown to affect osteoblasts *in vitro*. In low concentrations (2-4 mmol) Ca stimulates osteoblasts to proliferate whereas in medium concentrations it boosted cell differentiation and matrix mineralization. In high concentration (> 10 mmol) Ca ions were shown to be toxic to cells.<sup>[49]</sup> Soluble P was reported to promote expression of matrix 1a protein (MGP) which is an essential protein for bone formation.<sup>[49]</sup> It is well accepted that Si participates in the process of bone formation probably by inducing precipitation

of hydroxyapatite in the early stages of matrix mineralization.<sup>[46, 47]</sup> The only study that investigated the effect of Nb species on osteoblast-like cells (MC3T3-E1 cells) concluded that in a dose-dependent manner ( $3 \times 10^{-7}$  M) these ions induce differentiation and mineralization of osteogenic cells rather than adhesion and proliferation.<sup>[14]</sup>

While the solubility of ions and their effect on the cells provide an insight into the probable mechanism by which bioactive materials influence biological effects it is not without problems. It is important to take into account the fact that these ions will mostly be complexed in large molecules, thus, the observed effects of the glass-derived ions might actually be caused by the compounds of the elemental constituents of the glass rather than individual ions. Despite the specific ionic compounds formed after dissolving from the bioactive glasses not being well described they were shown to possess an overall effect over gene expression of osteoblasts.<sup>[50]</sup> Xinus *et al.*<sup>[50]</sup> prepared a bioactive glass conditioned medium containing 1% w/v of 45S5 Bioglass<sup>®</sup> in DMEM and filtered the medium to remove glass particulates (0.2  $\mu$ m filter). Thus, they treated human osteoblasts with this medium for 24 hours and performed cDNA microarrays to analyze gene expression. Their results showed that bioglass dissolution products were able to up-regulate many genes related to osteoblast metabolism, cell proliferation, cell-cell and matrix-cell adhesion up to 5 fold.<sup>[50]</sup>

Immediately after implantation the glass rod started to exchange ions with the body fluid, releasing ionic products that acted over osteogenic cells located in the adjacent periosteum and bone marrow. The glass dissolution products may have stimulated periosteal osteogenic cells to differentiate into polarized secretory osteoblasts that began to produce new bone onto the pre-existent bone promoting appositional bone growing forming a very clear cement line (arrows in **Figure 8**). This chain of events is believed to have happened for both glass compositions, as the two of them showed histological signs of subperiosteal bone formation. The comparison of subperiosteal bone area in the BGSN1 group and in the control group (BG45S5) showed significant larger bone area in the control

group after 28 days of implantation [ $F(3, 16) = 1.881, p = 0.174$ ] (**Figure 8**) despite both glasses clearly stimulating periosteal cells to differentiate and produce new bone.

The present study has gathered sufficient information to claim that substituting small concentrations of silicon dioxide with niobium pentoxide in 45S5 Bioglass® results in biomaterials that are cytocompatible with BM-derived MSCs and that are able to stimulate these cells to differentiate into osteoblast. Furthermore, we showed these new materials possess the bioactive properties of osteoconductivity and osteostimulation *in vivo*.

## **Conclusion**

This paper brings the investigation of biological properties of a novel bioactive glass in which silicon dioxide was partially substituted with niobium pentoxide. In sum, our results showed that when incubated in buffered solution the glass composition BGSN1 released similar amounts of Ca, Na, P, and Si compared to BG45S5. However, BGSN1 also released Nb into the solution. The Nb-containing glasses BGSN1 and BGSN2.5 exhibited the ability to form an apatite layer onto their surfaces, which is a sign of bioactivity. In addition, the immersion of BGSN1 and BG45S5 into complete culture media for 24 h significantly increases the surface's roughness. Furthermore, BGNb glasses are nontoxic to BM-derived MSCs, instead, BGSN1 stimulated greater cell proliferation after up to 4 days of treatment than the control group. The dissolution products of the glass compositions BGSN1 and BGNS2.5 are osteogenic as they differentiated BM-derived cells towards osteoblast lineage after 21 days of treatment. *In vivo* experiments showed that BGSN1 was osteoconductive enabling the formation of a bone layer onto its surface. In addition, BGSN1 stimulated the osteogenic cells of the periosteum to form bone (from a very clear cement line) which indicates good osteostimulative capacity for this glass composition even though it was lower than that stimulated by BG45S5. These results let us conclude that the addition of 1 mol% of Nb<sub>2</sub>O<sub>5</sub> substituted for SiO<sub>2</sub> in 45S5 Bioglass® generates a cytocompatible material with great bioactive properties with significant potential for biomedical applications.

## **Acknowledgments**

The authors acknowledge the use of the analytical instrumentation facility at Institute of Chemistry - University of Campinas, which is supported by the State of Paulo. This work was carried out with the support of the São Paulo Research Foundation – FAPESP (Grant: 2010/05394-9, 2010/12376-5, 2010/00863-0, 2011/09240-9 and 2011/17877-7) and The National Council for Scientific and Technological Development (CNPq/PIBITI) for the financial support. The authors would like to thank Brazilian Nanotechnology National Laboratory (LNNano) for technical support during SEM and AFM analyzes especially Dr. Carlos Alberto Rodrigues Costa for his technical assistance with AFM analysis.

## **Author Contributions**

J. H. L. and L. P. L. S. conceived and performed the experiments, analyzed the results, and wrote the paper. J. H. L. performed the spectroscopic observation. All authors reviewed the paper.

## **Additional Information**

Competing financial interests: The authors declare no competing financial interests.

## References

- [1] P. MV, Beata L-C, A. EN, et al. An overview of recent advances in designing orthopedic and craniofacial implants[J]. *Journal of Biomedical Materials Research Part A* 2013,101(11):3349-3364.
- [2] Jones JR, Brauer DS, Hupa L, et al. Bioglass and Bioactive Glasses and Their Impact on Healthcare[J]. *International Journal of Applied Glass Science (in English)* 2016,7(4):423-434.
- [3] Kushwaha M, Pan X, Holloway JA, et al. Differentiation of human mesenchymal stem cells on niobium-doped fluorapatite glass-ceramics[J]. *Dent Mater* 2012,28(3):252-60.
- [4] Ferreira FV, De Souza LP, Martins T, et al. Nanocellulose/Bioactive Glass Cryogel as Scaffolds for Bone Regeneration[J]. *Nanoscale* 2019.
- [5] Lopes JH, Mazali IO, Landers R, et al. Structural Investigation of the Surface of Bioglass 45S5 Enriched with Calcium Ions[J]. *Journal of the American Ceramic Society (in English)* 2013,96(5):1464-1469.
- [6] Lopes JH, Magalhaes JA, Gouveia RF, et al. Hierarchical structures of beta-TCP/45S5 bioglass hybrid scaffolds prepared by gelcasting[J]. *J Mech Behav Biomed Mater* 2016,62:10-23.
- [7] Lopes JH, Fonseca EMB, Mazali IO, et al. Facile and innovative method for bioglass surface modification: Optimization studies[J]. *Mater Sci Eng C Mater Biol Appl* 2017,72:86-97.
- [8] Lopes JH, Bueno OMVM, Mazali IO, et al. Investigation of citric acid-assisted sol-gel synthesis coupled to the self-propagating combustion method for preparing bioactive glass with high structural homogeneity[J]. *Materials Science and Engineering: C* 2019,97:669-678.
- [9] Jones JR. Reprint of: Review of bioactive glass: From Hench to hybrids[J]. *Acta Biomaterialia* 2015,23(S):S53-S82.
- [10] Hench LL, Jones JR. Bioactive Glasses: Frontiers and Challenges[J]. *Frontiers in Bioengineering and Biotechnology* 2015,3:194.
- [11] Hench LL, Polak JM, Xynos ID, et al. Bioactive materials to control cell cycle[J]. *Materials Research Innovations (in English)* 2000,3(6):313-323.
- [12] Hench LL. The story of Bioglass (R)[J]. *Journal of Materials Science-Materials in Medicine (in English)* 2006,17(11):967-978.
- [13] Lombardi M, Gremillard L, Chevalier J, et al. A Comparative Study between Melt-Derived and Sol-Gel Synthesized 45S5 Bioactive Glasses[J]. *Key Engineering Materials* 2013,541:15-30.
- [14] Obata A, Takahashi Y, Miyajima T, et al. Effects of niobium ions released from calcium phosphate invert glasses containing Nb<sub>2</sub>O<sub>5</sub> on osteoblast-like cell functions[J]. *ACS Appl Mater Interfaces (in English)* 2012,4(10):5684-90.
- [15] Denry IL, Holloway JA, Nakkula RJ, et al. Effect of niobium content on the microstructure and thermal properties of fluorapatite glass-ceramics[J]. *J Biomed Mater Res B Appl Biomater* 2005,75(1):18-24.
- [16] Lopes JH, Magalhães A, Mazali IO, et al. Effect of Niobium Oxide on the Structure and Properties of Melt-Derived Bioactive Glasses[J]. *Journal of the American Ceramic Society (in English)* 2014,97(12):3843-3852.
- [17] Cacciotti I, Lehmann G, Camaioni A, et al. AP40 Bioactive Glass Ceramic by Sol-Gel Synthesis: In Vitro Dissolution and Cell-Mediated Bioresorption[J]. *Key Engineering Materials* 2013,541:41-50.
- [18] De Bonis A, Curcio M, Fosca M, et al. RBP1 bioactive glass-ceramic films obtained by Pulsed Laser Deposition[J]. *Materials Letters* 2016,175:195-198.
- [19] Fernandes GVO, Alves GG, Linhares ABR, et al. Evaluation of cytocompatibility of bioglass-niobium granules with human primary osteoblasts: A multiparametric approach[J]. *Key engineering materials* 2012,493-494:37-42.
- [20] Wang X, Meng X, Chu S, et al. Osseointegration behavior of novel Ti-Nb-Zr-Ta-Si alloy for dental implants: an in vivo study[J]. *Journal of Materials Science: Materials in Medicine* 2016,27(9):139.

- [21] Ana Lúcia Roselino R, Peter H, Luís Geraldo V, et al. Are new TiNbZr alloys potential substitutes of the Ti6Al4V alloy for dental applications? An electrochemical corrosion study[J]. *Biomedical Materials* 2013,8(6):065005.
- [22] Mallick K. *Bone Substitute Biomaterials Elsevier Science*, 2014.
- [23] LOPES JH, BERTRAN CA, DE SLPL, et al. Composição vítrea bioativa e seu uso para regeneração óssea 2016.
- [24] Lopes JH. Biovidros derivados do 45S5: Os efeitos do Nb2O5 ou da modificação da superfície com Ca<sup>2+</sup> sobre a estrutura e bioatividade. *Universidade Estadual de Campinas - Instituto de Química* 2015; PhD.
- [25] Cacciotti I. Bivalent cationic ions doped bioactive glasses: the influence of magnesium, zinc, strontium and copper on the physical and biological properties[J]. *Journal of Materials Science* 2017,52(15):8812-8831.
- [26] Souza L, Lopes JH, Encarnação D, et al. Comprehensive in vitro and in vivo studies of novel melt-derived Nb-substituted 45S5 bioglass reveal its enhanced bioactive properties for bone healing[J]. *Scientific Reports* 2018,8(1):12808.
- [27] Hench LL. Bioceramics - From concept to clinic[J]. *Journal of the American Ceramic Society* 1991,74(7):1487-1510.
- [28] Hench LL, Wilson J. *An Introduction to Bioceramics World Scientific Publishing C. Pte. Limited*, 1993.
- [29] Hench LL, Splinter RJ, Allen WC, et al. Bonding mechanisms at the interface of ceramic prosthetic materials[J]. *Journal of Biomedical Materials Research* 1972,5(6):117-141.
- [30] Cacciotti I. Cationic and Anionic Substitutions in Hydroxyapatite. In: Antoniac IV, editor. *Handbook of Bioceramics and Biocomposites Cham: Springer International Publishing*, 2014:1-68.
- [31] Martin RA, Twyman H, Qiu D, et al. A study of the formation of amorphous calcium phosphate and hydroxyapatite on melt quenched Bioglass® using surface sensitive shallow angle X-ray diffraction[J]. *Journal of Materials Science: Materials in Medicine* 2009,20(4):883-888.
- [32] Lopes JH, Magalhaes A, Mazali IO, et al. Effect of Niobium Oxide on the Structure and Properties of Melt-Derived Bioactive Glasses[J]. *Journal of the American Ceramic Society (in English)* 2014,97(12):3843-3852.
- [33] Minghui T, Wenchuan C, Jun L, et al. Human Induced Pluripotent Stem Cell-Derived Mesenchymal Stem Cell Seeding on Calcium Phosphate Scaffold for Bone Regeneration[J]. *Tissue Engineering Part A* 2014,20(7-8):1295-1305.
- [34] Capanema NSV, Mansur AAP, Carvalho SM, et al. Niobium-Doped Hydroxyapatite Bioceramics: Synthesis, Characterization and In Vitro Cytocompatibility[J]. *Materials* 2015,8(7):4191-4209.
- [35] Mestieri LB, Gomes-Cornélio AL, Rodrigues EM, et al. Cytotoxicity and Bioactivity of Calcium Silicate Cements Combined with Niobium Oxide in Different Cell Lines[J]. *Brazilian Dental Journal* 2017,28:65-71.
- [36] Diomedea F, Gugliandolo A, Cardelli P, et al. Three-dimensional printed PLA scaffold and human gingival stem cell-derived extracellular vesicles: a new tool for bone defect repair[J]. *Stem Cell Research & Therapy* 2018,9(1):104.
- [37] Chen W, Liu J, Manuchehrabadi N, et al. Umbilical cord and bone marrow mesenchymal stem cell seeding on macroporous calcium phosphate for bone regeneration in rat cranial defects[J]. *Biomaterials* 2013,34(38):9917-9925.
- [38] Krishnamurthy G, Murali MR, Hamdi M, et al. Proliferation and osteogenic differentiation of mesenchymal stromal cells in a novel porous hydroxyapatite scaffold[J]. *Regenerative Medicine* 2015,10(5):579-590.
- [39] Wang C, Meng H, Wang X, et al. Differentiation of Bone Marrow Mesenchymal Stem Cells in Osteoblasts and Adipocytes and its Role in Treatment of Osteoporosis[J]. *Medical Science Monitor : International Medical Journal of Experimental and Clinical Research* 2016,22:226-233.

- [40] Lehmann G, Cacciotti I, Palmero P, et al. Differentiation of osteoblast and osteoclast precursors on pure and silicon-substituted synthesized hydroxyapatites[J]. *Biomedical Materials* 2012,7(5):055001.
- [41] Fernandez de Grado G, Keller L, Idoux-Gillet Y, et al. Bone substitutes: a review of their characteristics, clinical use, and perspectives for large bone defects management[J]. *Journal of Tissue Engineering* 2018,9:2041731418776819.
- [42] Shirin T, Nima B, Javad B. Nonunion fractures, mesenchymal stem cells and bone tissue engineering[J]. *Journal of Biomedical Materials Research Part A* 0(0).
- [43] Matsuno H, Yokoyama A, Watari F, et al. Biocompatibility and osteogenesis of refractory metal implants, titanium, hafnium, niobium, tantalum and rhenium[J]. *Biomaterials* 2001,22(11):1253-1262.
- [44] Bai Y, Deng Y, Zheng Y, et al. Characterization, corrosion behavior, cellular response and in vivo bone tissue compatibility of titanium–niobium alloy with low Young's modulus[J]. *Materials Science and Engineering: C* 2016,59:565-576.
- [45] Boyan B, Schwartz Z. Modulation of osteogenesis via implant surface design. *Bone Engineering* 2000: 233–239.
- [46] Steele J, Dalton B. Underlying mechanisms of cellular adhesion in vitro during colonization of synthetic surfaces by bone- derived cells. *Bone Engineering* 2000: 225–231.
- [47] Lakhkar NJ, Lee I-H, Kim H-W, et al. Bone formation controlled by biologically relevant inorganic ions: Role and controlled delivery from phosphate-based glasses[J]. *Advanced Drug Delivery Reviews* 2013,65(4):405-420.
- [48] Hoppe A, Guldal NS, Boccaccini AR. A review of the biological response to ionic dissolution products from bioactive glasses and glass-ceramics[J]. *Biomaterials (in English)* 2011,32(11):2757-2774.
- [49] Maeno S, Niki Y, Matsumoto H, et al. The effect of calcium ion concentration on osteoblast viability, proliferation and differentiation in monolayer and 3D culture[J]. *Biomaterials* 2005,26(23):4847-4855.
- [50] Xynos ID, Edgar AJ, Buttery LDK, et al. Gene-expression profiling of human osteoblasts following treatment with the ionic products of Bioglass® 45S5 dissolution[J]. *Journal of Biomedical Materials Research* 2001,55(2):151-157.

## ***Figure Captions***

**Figure 1.** ICP data: ion release vs. time in 50.69 mM HEPES solution at pH 7.40 for BG45S5 and Nb-substituted bioactive glass. The data displayed in (a), (b), (c) and (d) are related to leached Na, Ca, Si, and P species from glass derived from substitution of SiO<sub>2</sub> for Nb<sub>2</sub>O<sub>5</sub>.

**Figure 2.** ICP data: Nb ion release vs. time in 50.69 mM HEPES solution at pH 7.40 for BG45S5 and Nb-substituted bioactive glass. The amounts of niobium determined by ICP-OES is consistent with the niobium content in each sample, i.e. BGSN5 exhibits a higher peak of niobium concentration compared to the BGSN1 bioactive glass. As expected, no niobium was detected for BG45S5.

**Figure 3.** <sup>31</sup>P MAS-NMR spectra for the different glass compositions, recorded at a magnetic field strength of 9.4 T and a spinning speed of 10 kHz: (a) BG45S5, (b) BGSN1, (c) BGSN2.5, and (d) BGSN5. The chemical environmental for <sup>31</sup>P shifts progressively evolves to lower values of  $\delta$ , reaching a peak position similar to the <sup>31</sup>P spectrum observed in the hydroxyapatite control.

**Figure 4.** Micrographs of BM-derived MSCs treated for 72 h with culture media conditioned with the dissolution products of: BG45S5 (a), BGSN1 (b), BGSN2.5 (c), and BGSN5 (d) at a concentration of 10 mg·mL. Following the incubation period, a negative control of dead cells was established by incubating cells with 70% methanol for 30 min (e). Cells treated with regular growth media served as a positive control (f). Dissolution products of none of the glass compositions were toxic to the tested cell line. (g) Viability of bone-marrow-derived mesenchymal stem cells (BM-MSCs) after 4 days of treatment with different glass-conditioned media measured by MTT assay. DMEM was used as a positive control and cells killed with DMSO as negative control. Results are expressed in mean and SEM. One-way ANOVA followed by Tukey's test was used to compare the groups. None of the glass-conditioned media (BG45S5, BGSN1, BGSN2.5 and BGSN5) reduced cell viability in comparison with the control group (DMEM). The group BGSN1 showed significantly higher absorbance than DMEM ( $p=0.0014$ ) and BG45S5 ( $p<0.0001$ ) after 4 days, suggesting superior cell proliferation.

**Figure 5.** Micrographs of calcium deposits within and around BM- derived MSCs stained with alizarin red (1%) and osteocalcin immunofluorescence after 21 days of treatment with different media. The six superior squares show micrographs (100× magnification) of BM-MSCs in which the red aggregates are calcium deposits. Cells treated with osteogenic medium (OST) showed a fully mineralized matrix which meaning that most cells were in a late stage of differentiation to osteoblasts. Those cells treated with BGSN1 and BGSN2.5 showed matrix mineralization. The four inferior squares display laser scanning confocal micrographs of BMMSCs treated with BGSN1 showing osteocalcin immunofluorescence (in red), cell nuclei stained with DAPI (in bright blue), mineralized matrix by reflection of laser in TRANS mode (black) and an overlapping of matrix and nuclei.

**Figure 6.** Three-dimensional surface AFM images for an area of 30 x 30  $\mu\text{m}$  and SEM micrographs at magnifications of 3000x of bioactive glass 45S5 (a) before and (b) after 24 hours of immersion in complete culture medium; BGSN1 (c) before and (d) after 24 hours of immersion in complete culture medium showing the increase of surface roughness.

**Figure 7.** Micrographs of transversal histological sections of rats' tibias treated with glass rods for 28 days and stained Haematoxylin and Eosin at 100 and 400 x magnification. The glass implants were removed after decalcification to allow the preparation of the histological sections (empty areas marked with "Glass" are where the glass rods were located for 28 days), but, some fragments of the glass can still be seen (red arrows). The micrographs show the bone layer (marked with "\*") that formed around the glass implant. Images A and B illustrate the group treated with BG45S5 whilst images C and D represent rats treated with BGSN1. A t-student test showed no significant different between thickness

of the bone layer formed in the rats treated with BGSN1 and the control group (BG45S5) ( $p=0.9568$ ). For this analysis  $p<0.05$  was considered.

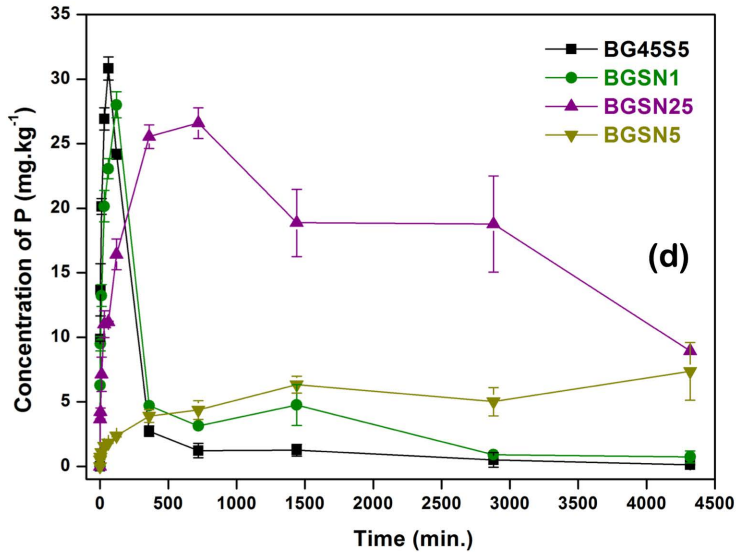
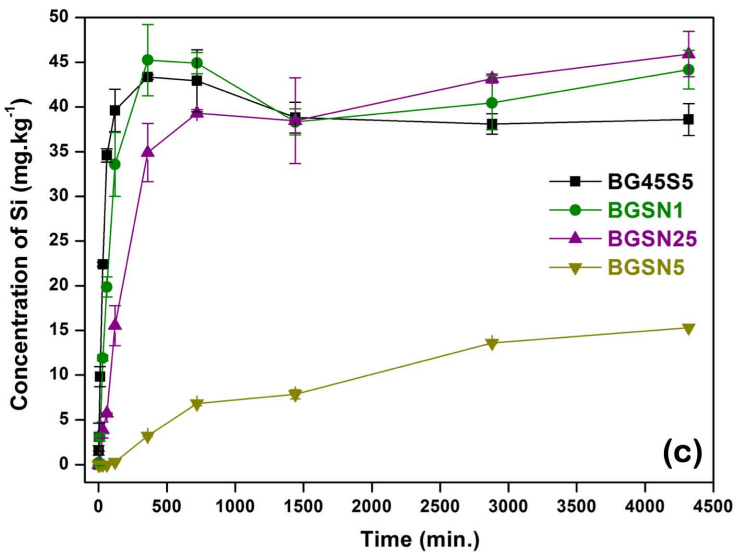
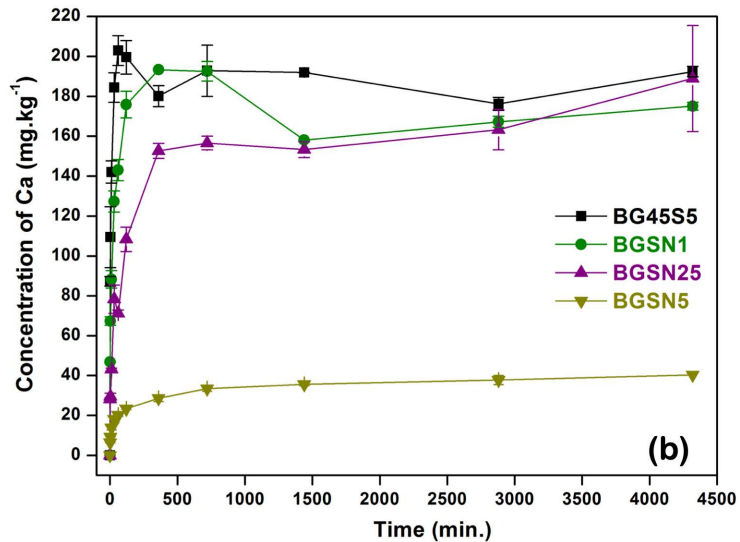
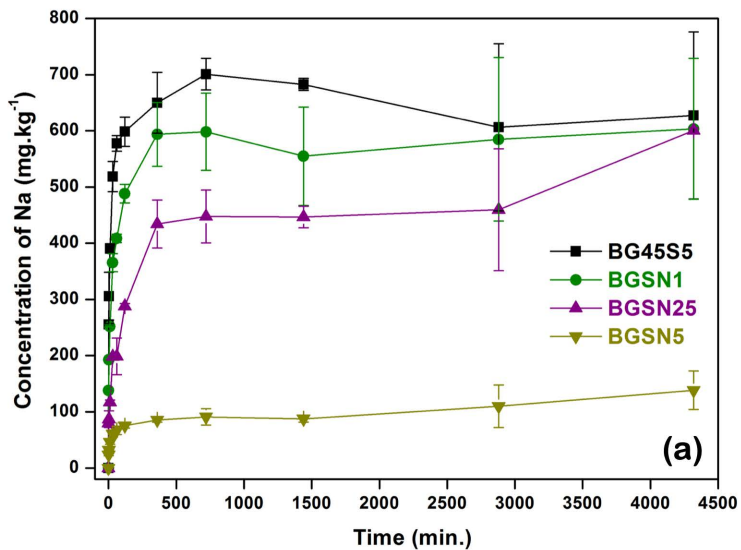
**Figure 8.** Micrographs of transversal histological sections of rats' tibias treated with glass rods for 28 days and stained Haematoxylin and Eosin at 100 and 400 x magnifications. The glass implants were removed after decalcification to allow the preparation of the histological sections (empty areas marked with "Glass" are where the glass rods were located for 28 days). The micrographs show the formation of bone by the osteogenic cells present at the inner layer of the periosteum (marked with an "\*"). The cement line (black arrows in images A and B) mark where the new bone started to form after the implantation of the material. Images A and B illustrate the group treated with BG45S5 whilst images C and D represent rats treated with BGSN1. A t-student test revealed that the group treated with BG45S5 ( $46469\pm 804.5\mu\text{m}$ ) presented a significantly larger sub periosteal bone area than the group treated with BGSN1 ( $40615\pm 1503\mu\text{m}$ ) ( $P=0.0085$ ). For this analysis  $p=0.05$  was considered.

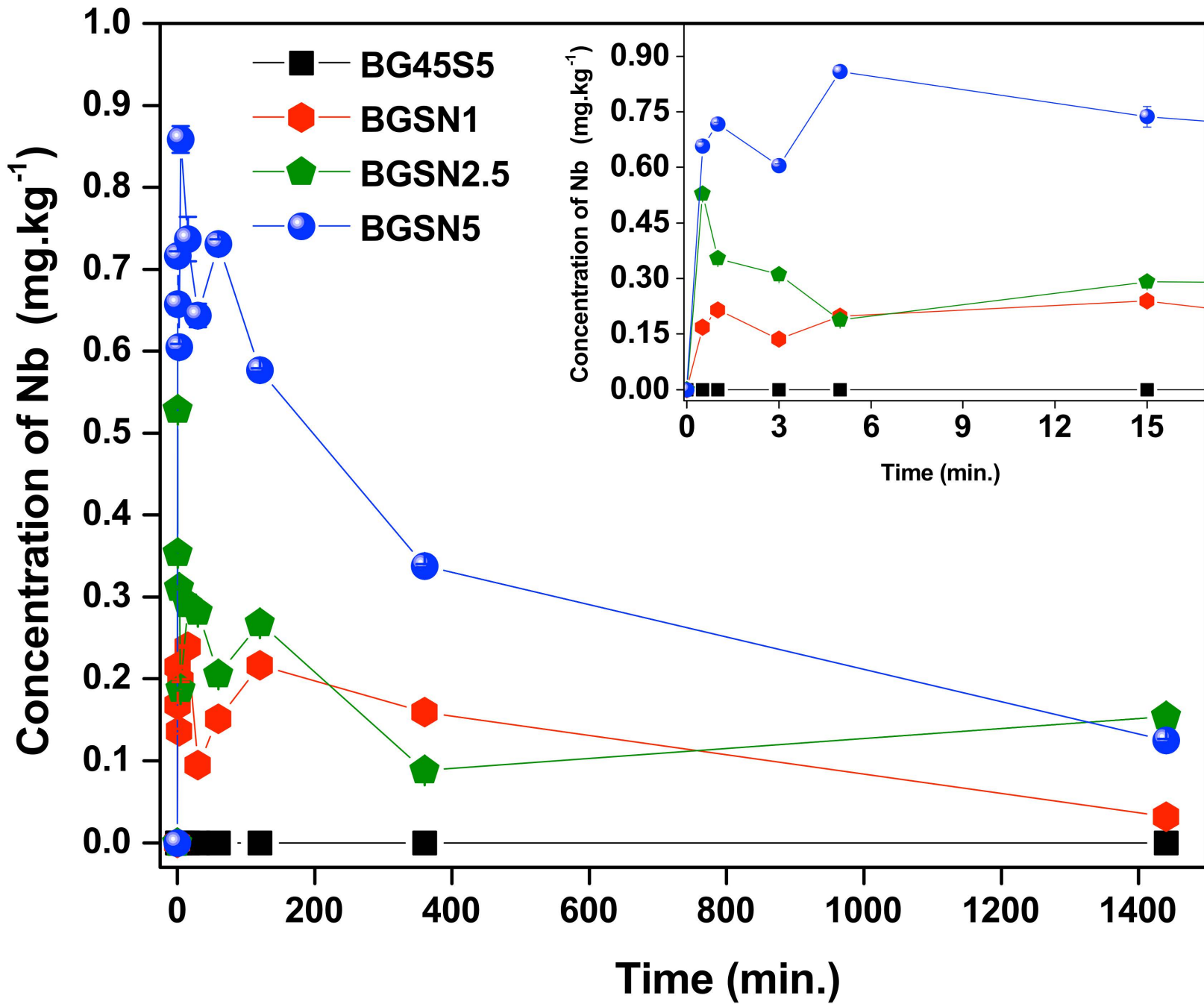
**Table 1** - Glass compositions (mol%) of BG45S5 and Nb-substituted 45S5 bioglass.

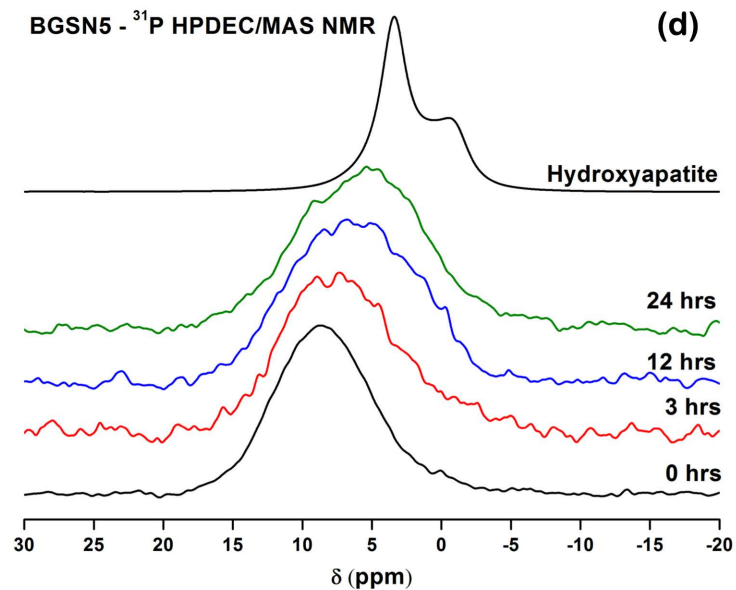
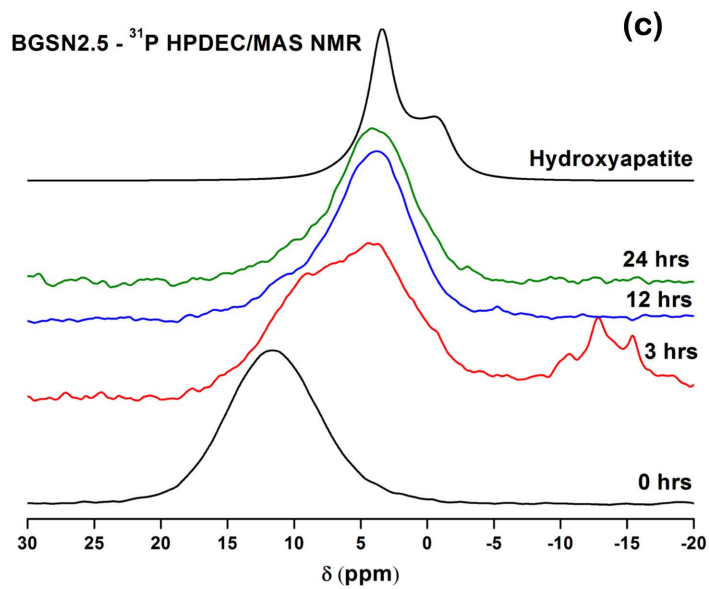
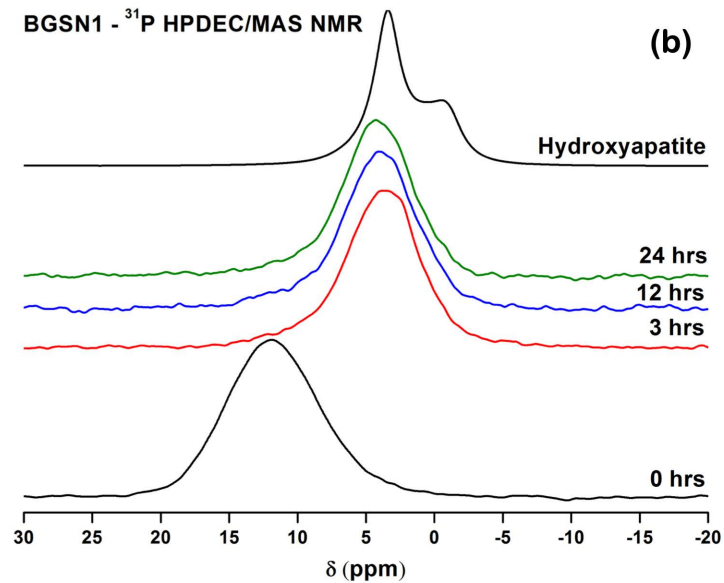
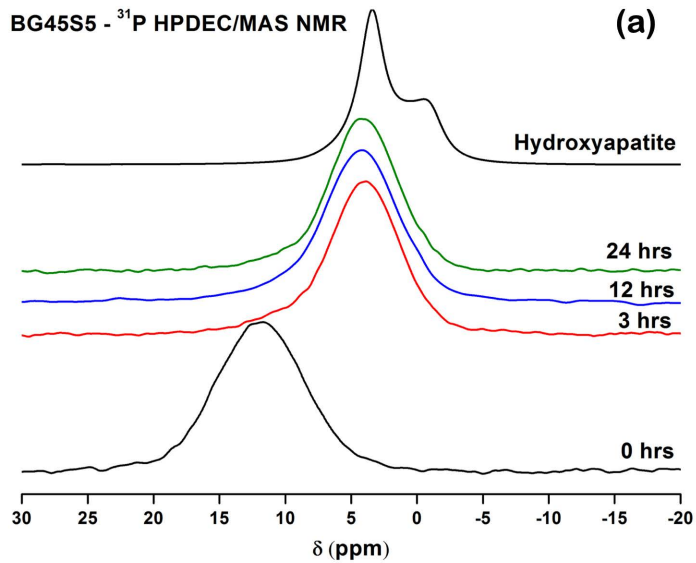
Glass	SiO <sub>2</sub>	CaO	Na <sub>2</sub> O	P <sub>2</sub> O <sub>5</sub>	Nb <sub>2</sub> O <sub>5</sub>
BG45S5	46.1	26.9	24.4	2.6	-
BGSN1	45.1	26.9	24.4	2.6	1.0
BGSN2.5	43.6	26.9	24.4	2.6	2.5
BGSN5	41.1	26.9	24.4	2.6	5.0

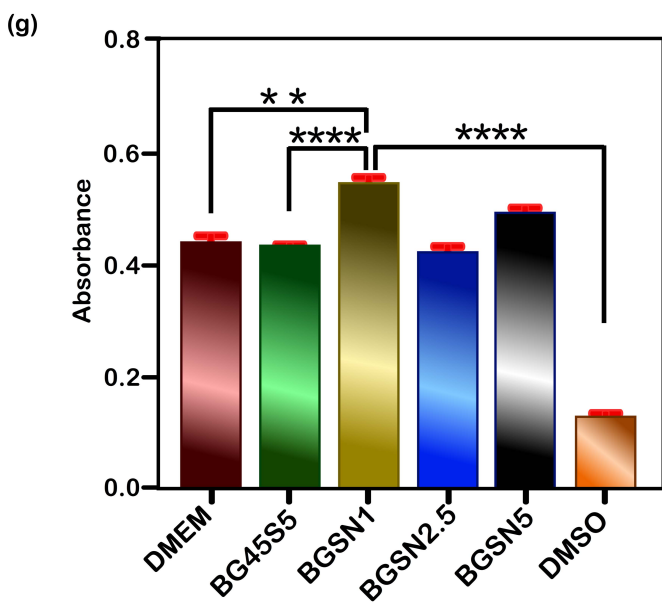
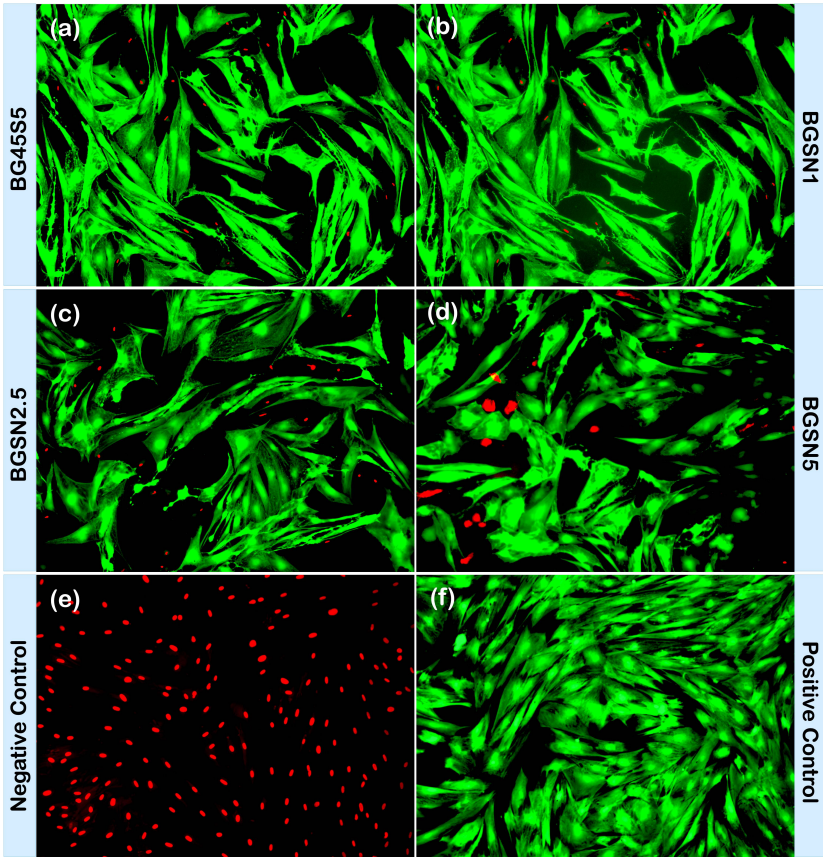
**Table 2** - <sup>31</sup>P MAS NMR peak positions and full width half maxima (FWHM) for BG45S5, Nb-substituted 45S5 bioglass and commercial hydroxyapatite.

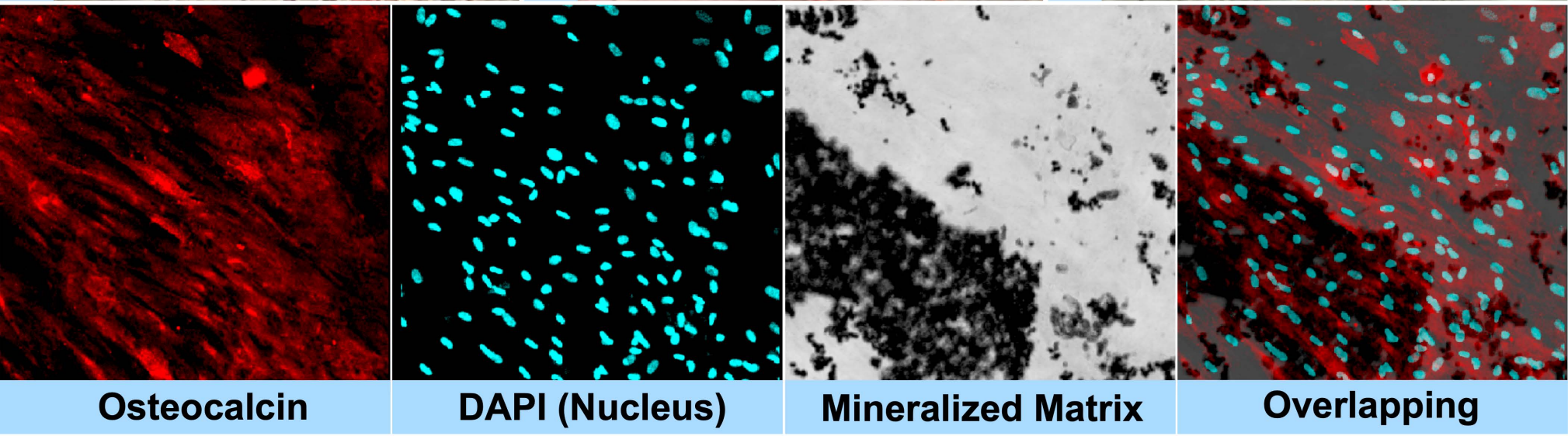
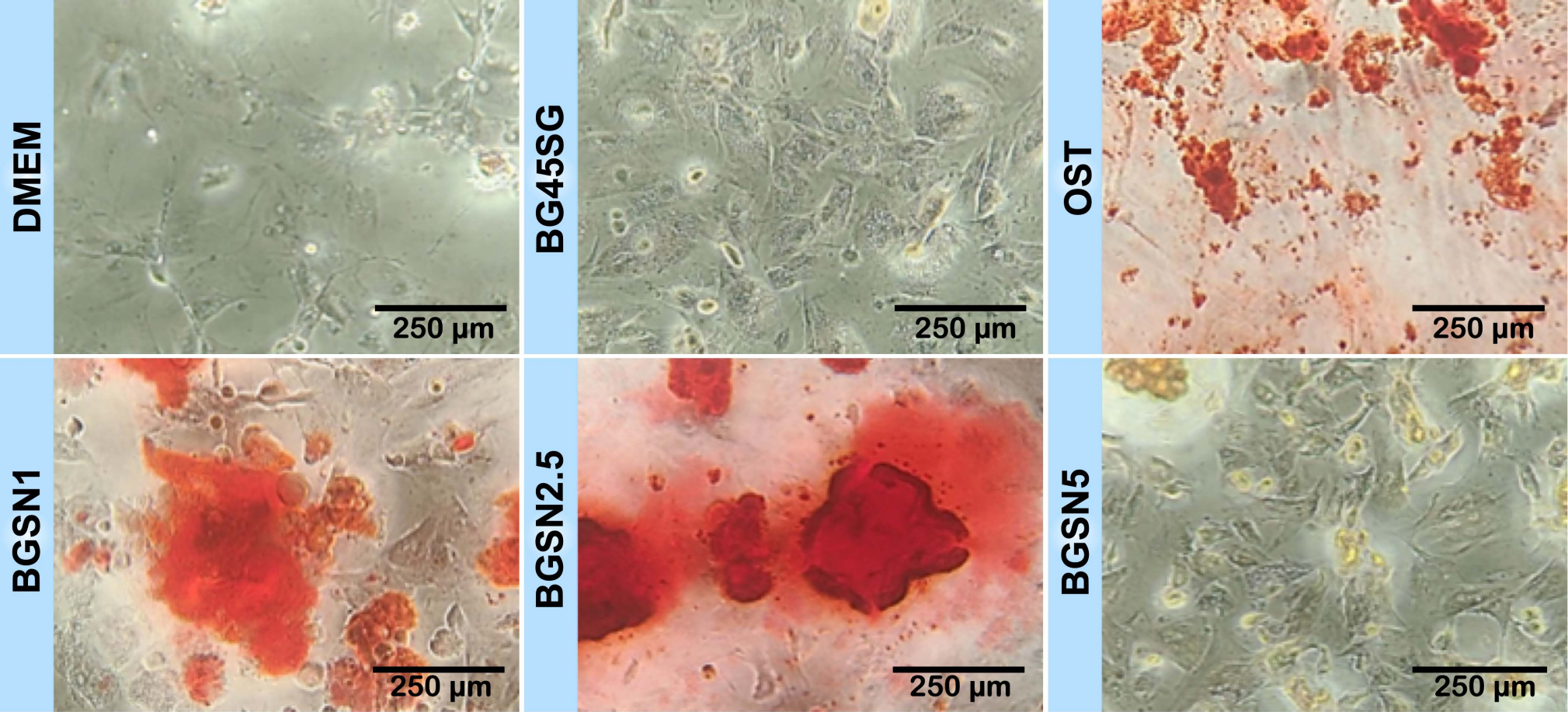
Glass	<sup>31</sup> P MAS NMR							
	Immersion time in SBF (hours)							
	0		3		12		24	
	Peak (ppm)	FWHM (ppm)	Peak (ppm)	FWHM (ppm)	Peak (ppm)	FWHM (ppm)	Peak (ppm)	FWHM (ppm)
BG45S5	11.9	7.9	4.0	6.2	4.3	6.6	4.0	6.1
BGSN1	11.8	7.9	3.8	5.9	3.9	6.1	4.1	5.9
BGSN2.5	11.6	8.0	5.7	11.8	4.3	7.2	4.1	7.2
BGSN5	8.5	8.1	7.4	9.7	6.3	11.4	5.7	10.7
<i>Reference</i>								
Hydroxyapatite	3.4	2.7	--	--	--	--	--	--



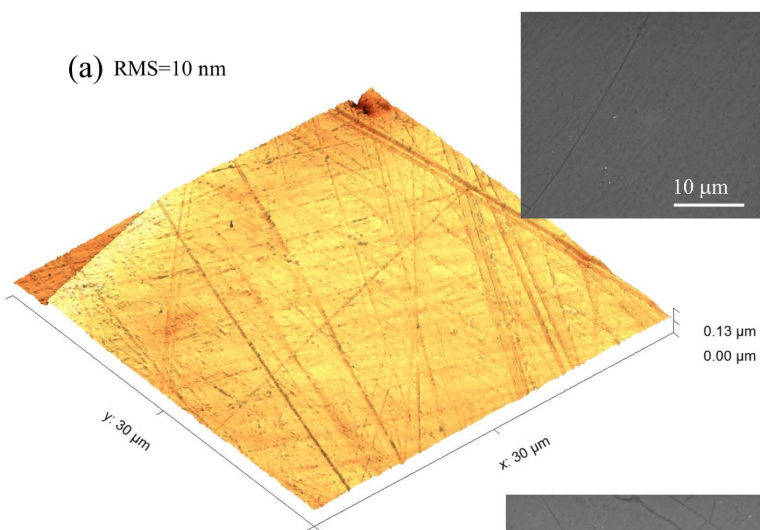




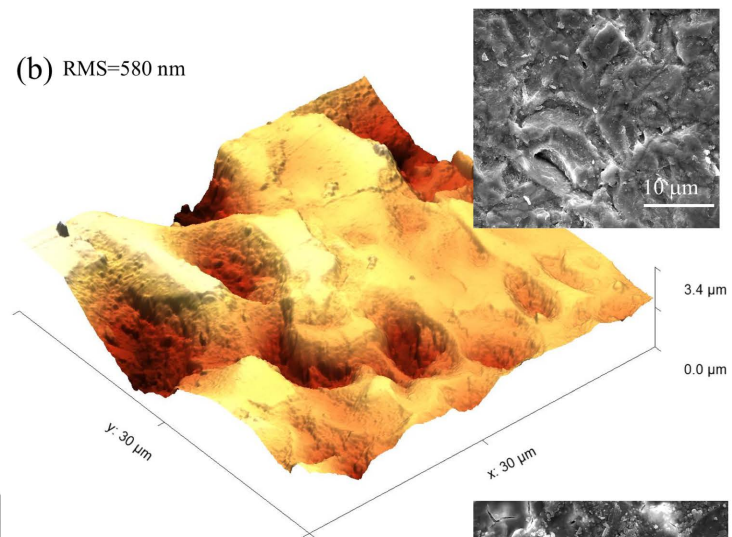




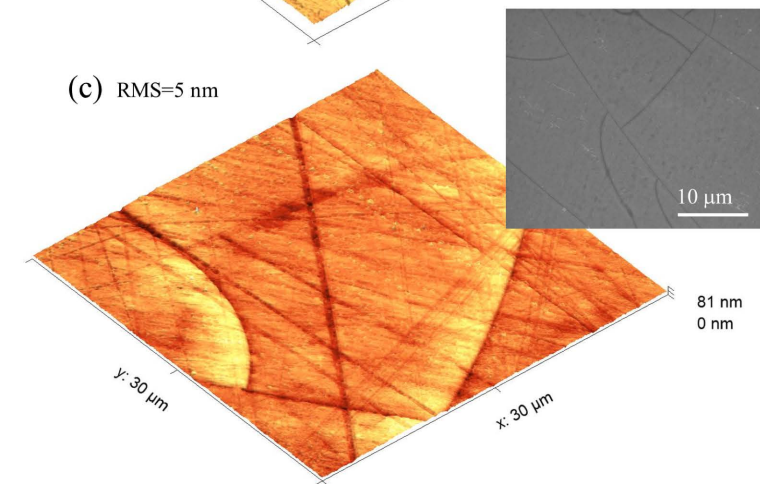
(a) RMS=10 nm



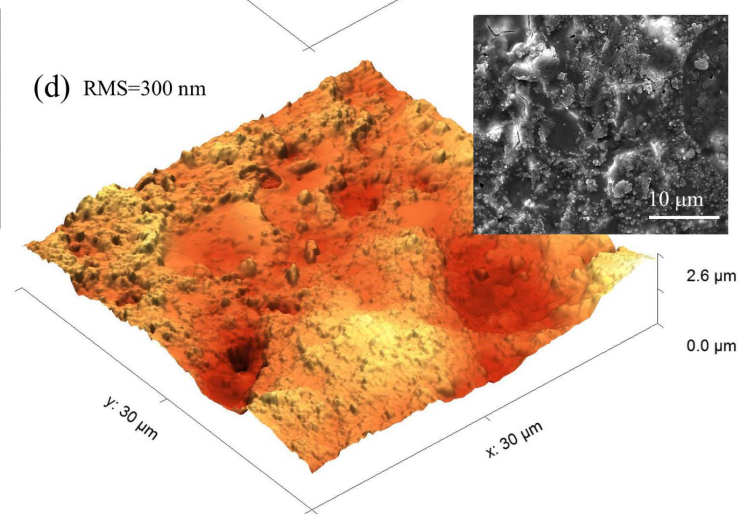
(b) RMS=580 nm



(c) RMS=5 nm



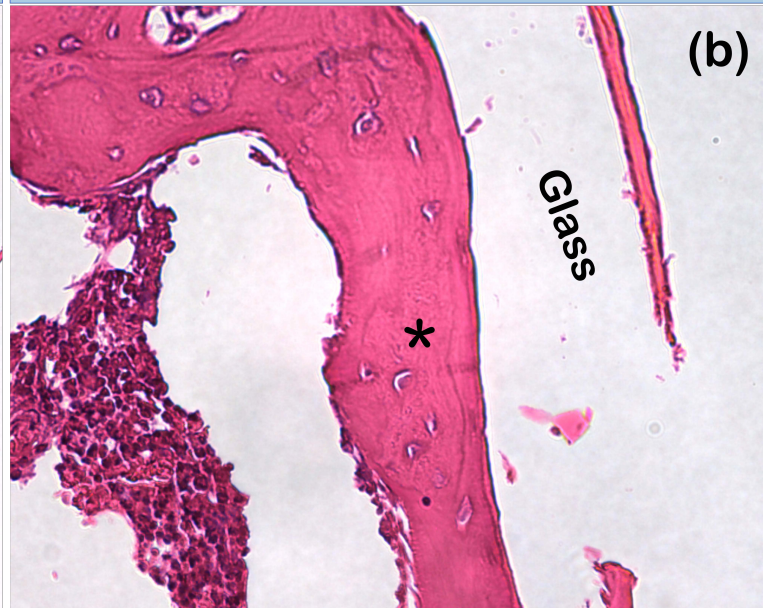
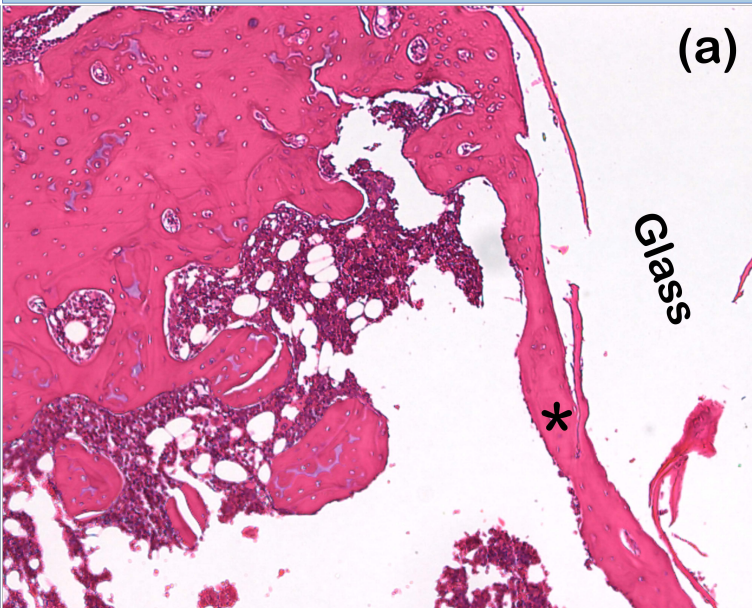
(d) RMS=300 nm



100x

400x

BG45S5



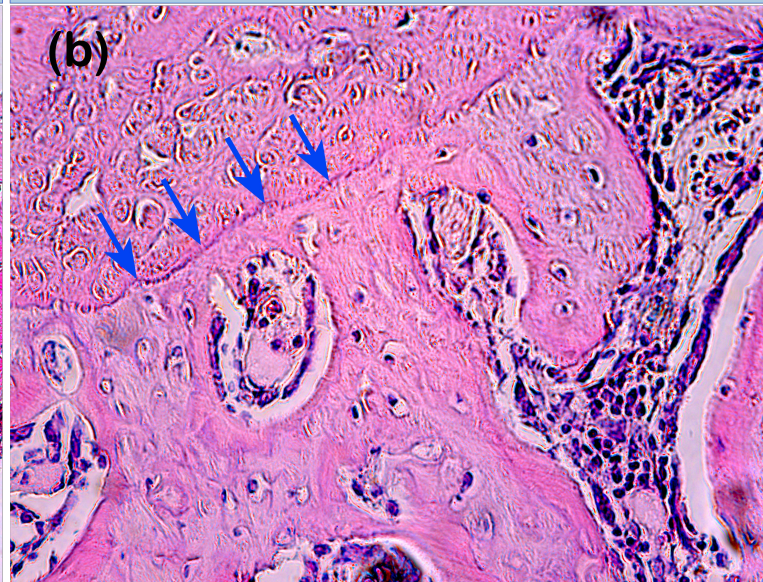
BGSN1



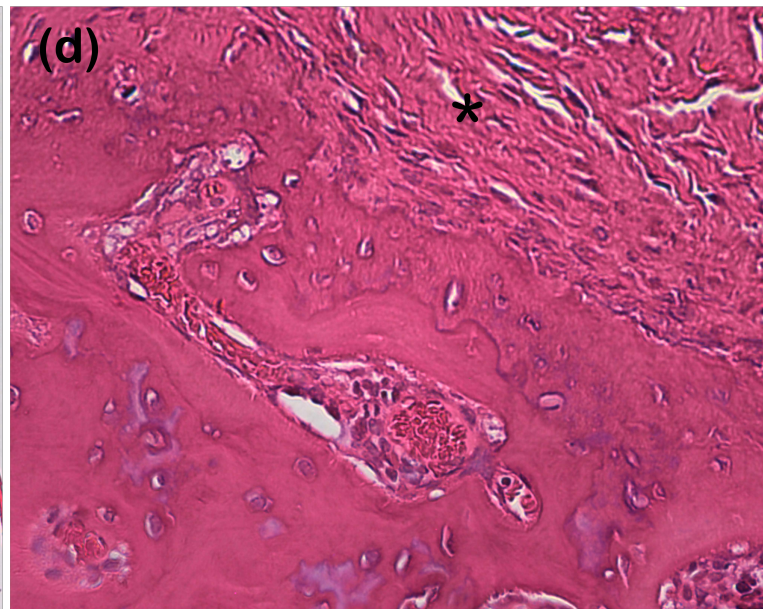
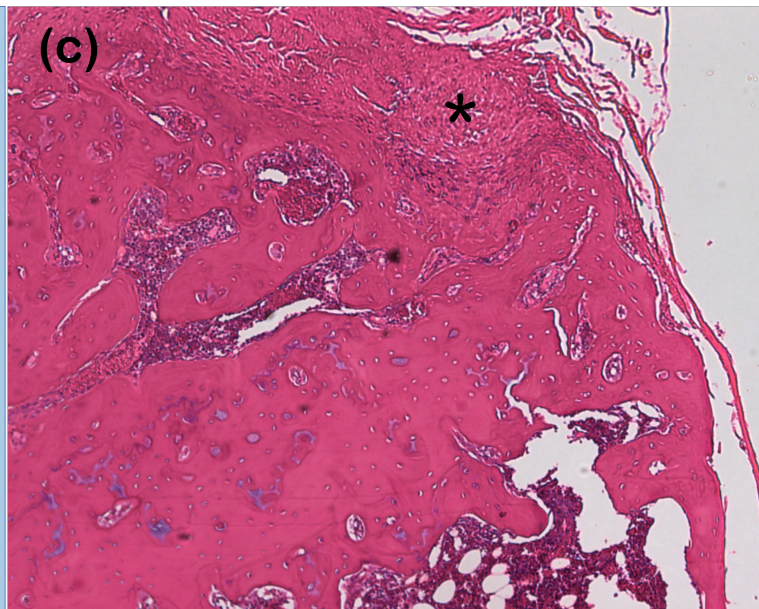
100x

400x

BG45S5



BGSN1



## Supplementary Material

### **In vitro and in vivo osteogenic potential of niobium-doped 45S5 bioactive glass: A comparative study**

*‡João H. Lopes\**, *‡Lucas P. Souza\**, *Juliana A. Domingues*, *Filipe V. Ferreira*, *Moema de Alencar Hausen*, *José A. Camilli*, *Richard A. Martin*, *Eliana Aparecida de Rezende Duek*, *Italo O. Mazali*, *Celso A. Bertran*.

#### AUTHOR INFORMATION

##### **J. H. Lopes**

Department of Chemistry, Division of Fundamental Sciences (IEF), Aeronautics Institute of Technology (ITA), 12228-900, Sao Jose dos Campos-SP – Brazil.

E-mail: ([lopes@ita.br](mailto:lopes@ita.br))

##### **L. P. Souza (corresponding author)**

Department of Structural and Functional Biology, Institute of Biology, University of Campinas – UNICAMP, 13083-862, Campinas, SP, Brazil.

E-mail: ([lpls2002@hotmail.com](mailto:lpls2002@hotmail.com))

##### **J. A. Domingues**

Department of Structural and Functional Biology, Institute of Biology, University of Campinas – UNICAMP, 13083-862, Campinas, SP, Brazil.

E-mail: ([almeidajad\\_bio@hotmail.com](mailto:almeidajad_bio@hotmail.com))

##### **F. V. Ferreira**

School of Chemical Engineering, University of Campinas - UNICAMP, 13083-970, Campinas, SP, Brazil.

E-mail: ([filipevargasf@gmail.com](mailto:filipevargasf@gmail.com))

##### **M. A. Hausen**

Department of Physiological Sciences, Biomaterials Laboratory, Pontifical Catholic University of São Paulo - PUC- SP, 18030-070, Sorocaba, SP, Brazil

E-mail: ([mahausen@pucsp.br](mailto:mahausen@pucsp.br))

##### **J. A. Camilli**

Department of Structural and Functional Biology, Institute of Biology, University of Campinas – UNICAMP, 13083-862, Campinas, SP, Brazil.

E-mail: ([jcamilli@unicamp.br](mailto:jcamilli@unicamp.br))

##### **R. A. Martin**

School of Engineering & Aston Research Centre for Healthy Ageing, Aston University, B47ET Birmingham, United Kingdom.

E-mail: ([r.a.martin@aston.ac.uk](mailto:r.a.martin@aston.ac.uk))

##### **E. A. R. Duek**

Department of Physiological Sciences, Biomaterials Laboratory, Pontifical Catholic University of São Paulo - PUC- SP, 18030-070, Sorocaba, SP, Brazil

E-mail: ([eliduek@pucsp.br](mailto:eliduek@pucsp.br))

**I. O. Mazali**

Department of Inorganic Chemistry, Institute of Chemistry, University of Campinas – UNICAMP, P.O. Box 6154, 13083-970, Campinas, SP, Brazil.

E-mail: ([mazali@iqm.unicamp.br](mailto:mazali@iqm.unicamp.br))

**C. A. Bertran**

Department of Physical Chemistry, Institute of Chemistry, University of Campinas – UNICAMP, P.O. Box 6154, 13083-970, Campinas, SP, Brazil.

E-mail: ([bertran@iqm.unicamp.br](mailto:bertran@iqm.unicamp.br))

*# These authors contributed equally.*

## SM1. Glass rods preparation

**Figure SM1** shows the experimental setup employed to prepare samples for in vivo assays.



**Figure SM1.** Devices used for the preparation of glass rods for in vivo tests: Graphite mould and suction system to force filling of the glass in the graphite mould. The vacuum pump was used to suction the molten glass, overcoming the high surface tension of the melt and allowing it to fill the 2 mm diameter graphite mould.<sup>[1]</sup>

**Figure SM2** shows a photograph of the glass rods used in the in vivo assays in the present work.

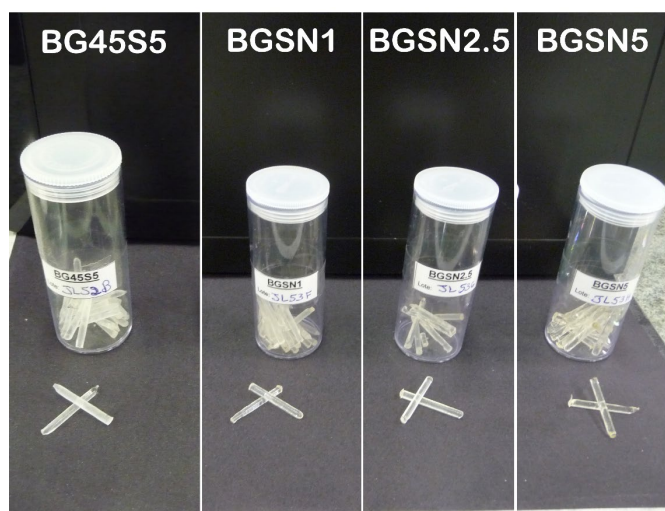


**Figure SM2.** Photograph of the glass rods used in the in vivo assays.

## SM2. Preparation of SBF solution

The acellular simulated body fluid (SBF) solution was prepared with concentrations of ions equal to those of blood plasma, including  $\text{Cl}^-$  and  $\text{HCO}_3^-$ . The pH value of 7.40 was obtained using the Hepes buffer at concentration 50.69 mmol/L. Details about the concentrations of the ions present in the SBF solution is presented in **Table SM1**.

**Table SM1.** Nominal ion concentrations of the SBF in comparison with those of human blood plasma.

Ions	Concentration/mM	
	Blood Plasma	SBF
$\text{Na}^+$	142.0	142.0
$\text{K}^+$	5.0	5.0
$\text{Mg}^{2+}$	1.5	1.5
$\text{Ca}^{2+}$	2.5	2.5
$\text{Cl}^-$	103.0	103.0
$\text{HCO}_3^{2-}$	27.0	27.0
$\text{HPO}_4^{2-}$	1.0	1.0
$\text{SO}_4^{2-}$	0.5	0.5

## SM3. Ion release in 50.69 mM HEPES solution at pH 7.40 for BG45S5 and Nb-substituted bioactive glass

**Figure SM3** shows a linear function with the square root of time up to about 120 min for all compositions.

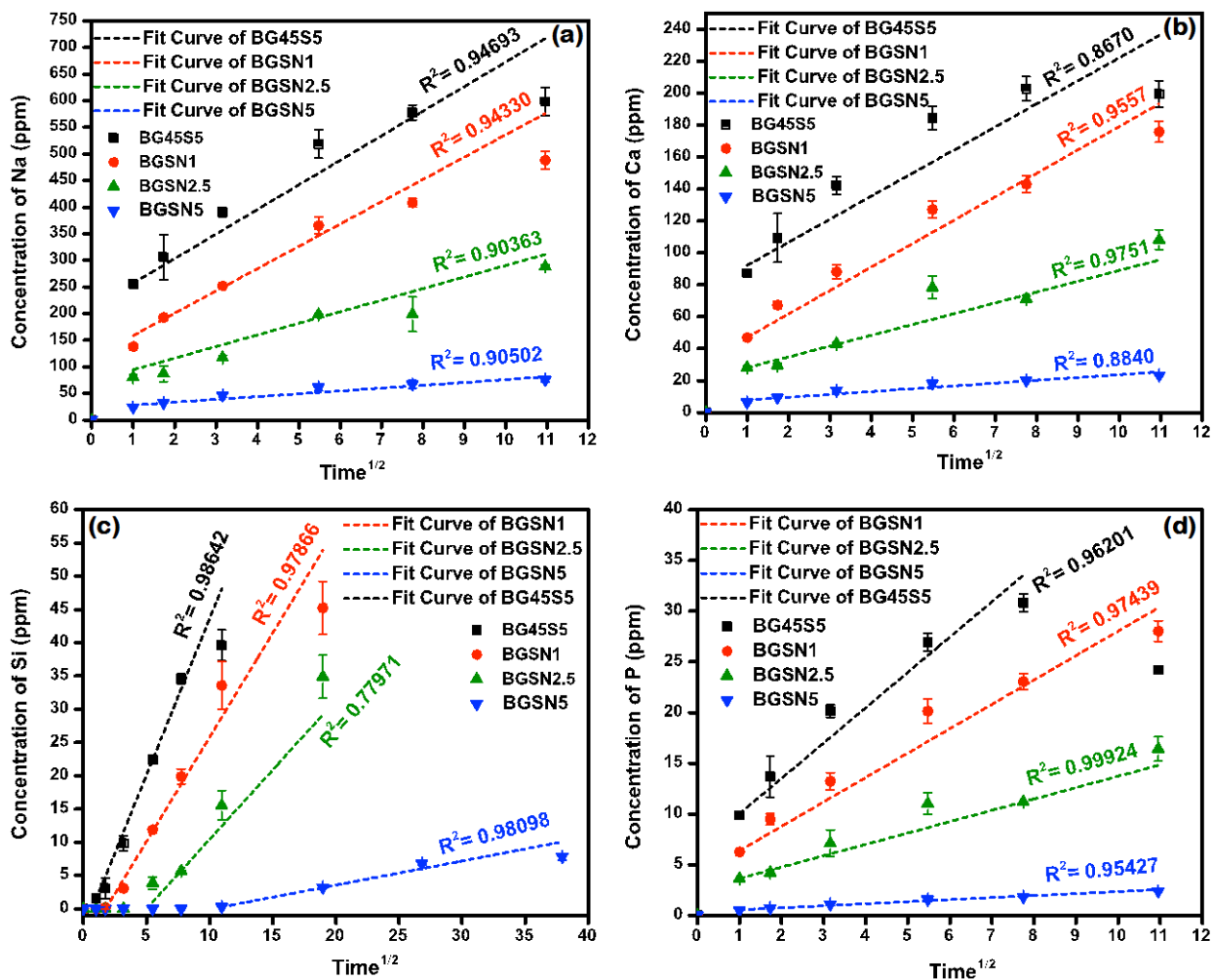


**Figure SM3.** ICP data: ion release as a function of square root of time in 50.69 mM HEPES solution at pH 7.40 for BG45S5 and Nb-substituted bioactive glass. The data displayed in (a), (b), (c), and (d) are related to leached of Na, Ca, Si, and P species, respectively, from glass derived from substitution of SiO<sub>2</sub> by Nb<sub>2</sub>O<sub>5</sub>. Lines are linear regression of dissolution data up to 120 min.

The elemental concentrations of sodium, calcium, silicon, and phosphorus exhibited a linear function of the square root of time up to about 120 min for all compositions, which indicates a two-step degradation mechanism with initial dissolution controlled by diffusion (exhibits a  $t^{1/2}$  dependence).

[1] Souza L, Lopes JH, Encarnação D, et al. Comprehensive in vitro and in vivo studies of novel melt-derived Nb-substituted 45S5 bioglass reveal its enhanced bioactive properties for bone healing[J]. *Scientific Reports* 2018,8(1):12808.